A river's connective tissue: Lab observations of particle pathways and riffle formation during floods

by

Lukas Mueller

A thesis

presented to the University of Waterloo

in fulfillment of the

thesis requirement for the degree of

Master of Applied Science

in

Civil Engineering (Water)

Waterloo, Ontario, Canada, 2023

Author's Declaration

I hereby declare that I am the sole author of this thesis. This is a true copy of the thesis, including any required final revisions, as accepted by my examiners.

I understand that my thesis may be made electronically available to the public.

Abstract

In rivers it is difficult to quantify bedform dynamics during storm events. Direct observation of sediment pathways would provide insight into the mechanisms that underly bedform formation and destruction. In the current study, our objective was to visualize these processes in a meandering pool-riffle system with partial bed cover. Observing erosive and depositional patterns, as well as the locations of active sediment transport, provides insight into the validity of various pool-riffle maintenance theories. We used a physical 1:40 scaled model of Toronto's Wilket Creek to simulate storm events during which riffles formed as connective bedforms between alternate point bars. Exported sediment was weighed and sieved to measure the grain size distribution, while the bed's pre- and post- storm topography was quantified using Structure-from-Motion techniques. Sediment pathways were observed using a novel technique, where regions of interest were filmed at 60 frames per second under ultra-violet light, illuminating painted tracers. Three paint colors were used for different size tracers, which allowed us to apply image segmentation and create separate videos for three size fractions of the sediment. Pathways were then extracted using Lagrangian tracking software. Results show that the area of active transport is limited to a narrow portion of the channel width that increases with flood stage. At low flow, transport is routed along the toe of point bars, while no particles travel into the region of the pool, where the bed is uncovered. Riffles are rarely observed at these stages. As the flow increases, the lateral extent of active transport expands to include the higher parts of the bars, while connective riffles grow in areal extent and height. Erosion and deposition was found to occur more readily along the active sediment transport zones. Pathways varied by particle size so that smaller particles traveled higher over the point bar and large particles tended to collect in the riffle. These results indicate that sediment-routing is a dominant mechanism behind the formation and maintenance of riffles in meandering rivers. Future work to quantify these processes will increase the effectiveness and longevity of river remediation design through targeted sediment augmentation instead of bedform reconstruction.

Acknowledgements

This thesis would not have been possible without help from my research group, my supervisor, my peers, and the technicians who helped me along the way. I would like to specifically acknowledge Megan Iun, who wrote most of the code used for data analysis, and Mark Hummel, who ensured that all of the flume experiments run smoothly.

Dedication

This thesis is dedicated to every teacher I have learned from, including – most importantly – my parents.

Table of Contents

List of Figures

List of Tables

Chapter 1 Introduction

1.1 Motivation

A river's bed can take many shapes, from wide and shallow fast-flowing regions called riffles, to deeper, slow-flowing regions called pools, often flanked by unsubmerged deposits of material called point bars. The mechanisms responsible for the organization of these river forms are difficult to investigate and understand, primarily due to the large number of variables at play and difficulties in their measurement. Increases in flow and depth during storm events alter the speed and direction of flowlines, while submerging areas that are dry during low flow. The distribution of shear force on the bed shifts, in turn changing the amount of sediment transported and the areas in which localized erosion and deposition occur. Due to the danger involved in observing the riverbed during these storm events, researchers are often resigned to performing investigations before or after the storm. However, observing the way in which these mechanisms interact with one another during storms is critical for understanding the time in which a river changes the most.

One way these issues have been addressed is by creating scaled down models of rivers and placing them into flumes or stream tables. Flumes are apparatuses that can control and measure flow and sediment rate entering and leaving the system. Although simplifications are present in all scaled down physical models, important underlying patterns can still be identified if these simplifications are accounted for in analysis, as shown by Tal & Paola (2010) in their study on how vegetation can reorganize a braided channel into a single-thread channel, or by McArdell & Wilcock (1993) in their flume study on how incipient motion – the threshold of force imparted on a particle before it moves – of a given particle size is linked to that size's total sediment transport.

A process that has long been described as imperative for how some rivers shape themselves is pool-riffle maintenance (De Almeida & Rodriguez, 2011; Hassan et al., 2021; Bayat et al., 2017). Pools, which are topographic lows conveying water in a slower, deeper manner, are often described as zones where sediment entrainment outweighs sediment deposition (Leopold & Wolman, 1960). The opposite is the case in riffles, characterized by their relatively high elevation due to the build up of sediment (Sawyer et al., 2010; Chartrand et al., 2018). Although morphologic differences between pools and riffles are clear, the mechanisms responsible for maintaining pool-riffle systems are unclear, in spite of the fact that several viable theories have been presented. The variability of pool-riffle systems adds to the complexity; some systems are fully alluvial, where the entirety of the bed

has the potential to become entrained by flow, while some systems are semi-alluvial, where a small layer of sediment overlays an immovable layer of bedrock, till, or even concrete (Polvi, 2021). Other sources of variability between pool-riffle systems includes each system's slope, stream power, grain size distribution, and degree of urbanization (MacVicar & Thompson, 2023; Bevan et al., 2018).

Several theories outlining the mechanisms that maintain pool-riffle systems have been proposed. Keller's velocity reversal theory has arguably been the most popular (Keller, 1971), with several subsequent theories building on the velocity reversal theory by introducing near-bed shear stress or near bed velocity reversals (Caamaño et al., 2009; Lisle, 1979; Booker et al., 2001). Others argued against the relevancy of velocity reversals in pool-riffle maintenance, positing that sediment transport does not occur in zones where reversals do, and if they were to, the reversals would not be sufficient in maintaining the entire system. Instead, other ideas involving the location of sediment pathways and the convergence and divergence of flow were introduced as replacement theories (Milan, 2013; MacWilliams et al., 2006; White et al., 2010). Information regarding the pathways that particles take in river bends would add valuable insight to the ongoing conversation regarding pool-riffle maintenance. Understanding how pools and riffles are maintained in a natural environment allows for the development of nature-based restoration designs, ensuring that they are robust and functional in a natural environment. Specifically, defining active transport zones would effectively narrow the scope of future studies concerning pool-riffle maintenance by identifying *where* key mechanisms occur throughout the channel, such that investigations regarding *how* they occur can be more targeted. The idea of using sediment augmentation to restore channel morphologies is attractive, as it utilizes a more temporally robust, cheaper, and nature-based solution when compared to alternative methods, such as site-specific bedform reconstruction.

1.2 Objectives

The goal of this study is to describe the movement of sediment through pool-riffles in a meandering channel, and the mechanisms behind the maintenance of riffles during floods. A flume study is used to allow for the observation of variables that would be difficult to measure in a real-world environment, such as the sediment's active transport zone, transport speed, and the evolution of bedforms. In addition to providing an evaluation of particle pathways, other data related to sediment transport such as sediment storage, fractional sediment export, channel hypsometry (distribution of sediment thickness), and bedform topography will be presented and analysed in order to provide a

more complete picture. The study will conclude by comparing and contrasting theories revolving around pool-riffle maintenance using the results from experimentation and will use the discussed ideas to assess the viability of river restoration via sediment augmentation, as a replacement for bedform reconstruction.

1.3 Scope

In this study, a natural channel morphology was created by routing sediment-laden water over an empty bed. The resulting topography was then subjected to a series of floods and observed after each experiment. After each flood, an experiment employing steady flow and sediment was performed, effectively resetting the bed before another flood event was run. In addition, several flood experiments were performed in sequence without resetting the bed in order to investigate the effects of sediment starvation.

Complete results from all experiments were included with exception of the particle tracking results. Although videos were recorded for all experiments conducted, one candidate experiment was chosen to highlight the perceived novelty and importance of the results and the method. The research was completed in parallel with methodological development of a novel particle tracking method that has not yet been published (Iun et al, in preparation). The results presented with this method are therefore somewhat preliminary. A rich dataset is available due to this study, warranting further analysis that is beyond the scope of this thesis.

Following the introduction, Chapter 2 contains a literature review, which begins with a high-level summary of the mechanisms involved with flow through river bends, before comparing existing theories on how pool-riffle systems are maintained. This examination will be followed by a review of previous flume experiments, outlining their methodologies and results, and how these relate to this study. In Chapter 3, the methodologies followed during experimentation and the analysis of results will be described. After presenting the results in Chapter 4, a discussion on their implications for the reproducibility of flume experiments, the validity of pool-riffle maintenance theories, and restoration efforts are presented in Chapter 5. Chapter 6 concludes this thesis, summarizing important points made.

Chapter 2 Literature Review

The way in which pools and riffles are maintained in a natural river involves the interaction of several individual mechanisms, making it a complex phenomenon that is, to this day, not fully understood. Most theories involve the idea that larger particles are mobilized by increases in flow and depth, occurring during storms (Keller, 1971; Milan, 2013). However, the path that sediment takes through the channel during storm events, as well as the timeline of events, is disputed. Shedding light onto these facts would allow for river engineers to integrate natural mechanisms into their design.

Although spatial patterns of topography and the organization of particle sizes in alluvial rivers have been observed (Montgomery & Buffington, 1997; Church & Ferguson, 2015), the mechanisms behind these patterns are not completely clear. Many theories behind how pool-riffles form in river bends have been suggested, supported by lab or field experiments, yet several valid theories remain in conflict with one another (MacVicar & Thompson, 2023). After outlining flow through bends, this section will provide background on two popular theories behind the mechanisms of pool-riffle maintenance: Keller's velocity reversal theory (1971) and Milan's sediment routing theory (2013). Various observations of other laboratory experiments performed previously on pool-riffle models are also included. Their findings are summarised and potential research gaps in both scope and apparatus are identified. These research gaps were a key motivator behind developing a methodology that is capable of tracking individual particles and of running unsteady flow through the model.

2.1 Flow in River Bends

On an increasing timescale, bedform evolution in rivers tends towards a meandering pattern. In his 1954 paper outlining the velocity distribution and boundary layer in channel bends, Hans Albert Einstein provides a theory that predicts the flow patterns in channel bends, based off the hydraulic equilibrium distribution within the bend. When looking at the velocity distribution of a natural channel, the higher velocities at the surface result in a 'spillover' phenomenon, effectively creating a vortex that travels outwards on the surface and inwards near the bed. This vortex forms above the thalweg and provides reasoning behind the movement of sediment from the outer, upstream bar to the inner, downstream bar (Einstein, 1954). Other recently published mathematical models show similar results, such as Ottevanger et al. (2002), and Blankaert (2011).

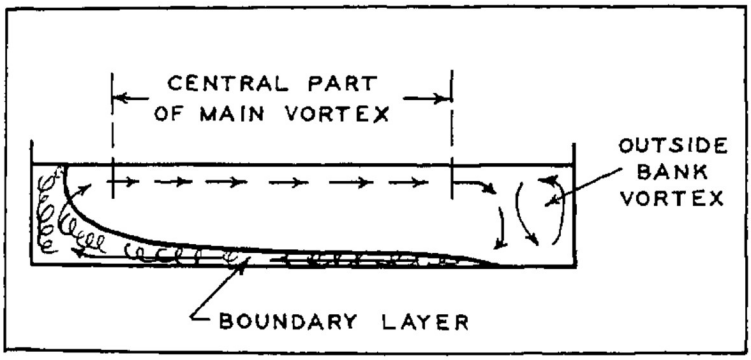

Figure 1. Depiction of vortex forming in a channel bend (Fig. 2 in Einstein, 1954)

Several laboratory studies focusing on flow patterns in flumes have also been performed. In Kashyap et al. (2012) a steady finite-volume 3D model was compared to flume results, where velocity profiles were developed for a 135º bend. Helical patterns were observed in both methods, clearly showing how flow lines at the surface were directed towards the outside bank of the channel, while flow lines near the bed were returning towards the inside of the bend. These circulatory cells were found to become more defined in sharper bends.

While studying meander development in bedrock channels, Turowski (2018) concluded that active meandering occurs when the outside banks of bends are eroded over time. Results from a model relying on sediment-flux-driven erosion concepts indicate that the erosion responsible for a greater degree of meandering continues until a state of equilibrium is established (Turowski, 2018). At this point, the rate of erosion on the outside bend would slow, and mechanisms causing meandering would cease. To make sense of these results, Turowski hypothesized that outer bank erosion, and thus meandering, is in part driven by particle impacts. These particles deflect from their original path, and, through inertial forces, travel tangentially away from the thalweg of the channel, impacting the outer wall and expediting erosion. A schematic of particle pathways through a meander bend is shown in Figure 2 (Turowski, 2018). The channel would reach a state of equilibrium once the outer bend has eroded to a degree where the flow no longer has the capability of forcing particles against the outer wall. As several assumptions made in the models used remain untested, Turowski calls for detailed investigations into the sediment dynamics of partially alluvial bedrock channels, especially those producing maps of particle activity within bends.

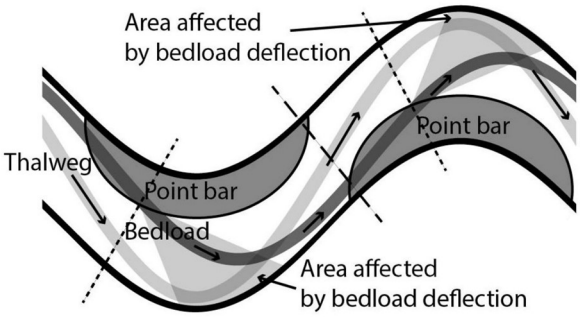

Figure 2. Depiction of bedload deflection towards the outside bank (Turowski, 2018)

2.2 Velocity Reversal Theory

Edward Keller, seeking to explain the mechanism behind the pool-riffle pattern found in many rivers, proposed the velocity reversal theory (1971). At low flow, the velocity of the flow over riffles is faster than the velocity at the bottom of pools. When discharge increases, the velocity at the bottom of the pool increases faster than the velocity over the riffle, effectively conveying large bedload into – and subsequently through – the pool. At the same time, velocity over the bed of the riffle decreases relative to the pool's bed, allowing larger bedload to deposit on the riffles. This sorting mechanism would occur over long periods of time, resulting in coarser material riffles and finer material pools.

Using a computational fluid dynamics approach coupled with observations from a field study, Booker et. al. (2001) sought to determine whether hydraulic reversals, or other patterns in boundary shear stress, play a role in pool-riffle maintenance. In all four pool-riffle sequences analysed, flow lines originating from the middle of riffles were routed away from the pools. When comparing these flow lines with tracer pathways, it is evident that the direction of near bed flow plays a large role in the movement of large particles. This study also investigated the effects of reversal flow structures on sediment transport through pool riffle systems. It was hypothesized that reversal zones located at the head of pools result in higher near bed velocity at the tail of the pool, effectively contributing to forces that transport sediment out of the pool. However, reversal flow structures were only found in one of four pool-riffle sequences, indicating that they are not necessary for pool-riffle maintenance.

In a paper analyzing the effects of variable channel geometry on the prevalence of velocity reversals (Byrne et al., 2021), velocities in 171 reaches throughout Northern California were surveyed. The goal of the study was to determine the frequency of velocity reversals in pool-riffle couplets, and to

determine the underlying mechanisms that cause them. To determine whether a reversal occurred, the width-to-depth ratios are compared to the Caamaño criterion – a threshold that, if exceeded, indicates that a velocity reversal should occur due to the conservation of mass (Caamaño et al., 2009). The Caamaño criterion was exceeded in 18% of pool-riffle systems studied, showing that reversals as defined by Caamaño are relatively infrequent.

Following the publication of Caamaño et al.'s (2009) reversal criterion theory, a discussion of the underlying assumptions made during the study was initiated by MacVicar et al. (2010). The discussion critiqued the use of bulk velocity in Caamaño et al.'s (2009) study, stating that partial reversals occurring near the bed may not be apparent in this type of observation. This argument was supported by measurements made by MacVicar et al. (2010) where near-bed reversals were apparent while bulk velocity reversals did not occur. In a similar vein, a study on a pool-riffle couplet in Moras Creek (MacVicar & Roy, 2007) found that significant reversals occurred near the bed in the pool's tail. Other mechanisms behind pool-riffle maintenance are also noted as significant, including fluid acceleration due to lateral flow convergence or high turbulence intensities. Alternately, Dashtpeyma & MacVicar (2023) suggest that the presence of post-riffle plunging flow can cause local zones of high velocity near the pool's bed.

Keller's results from one-dimensional modeling and the field study performed in Dry Creek, California, were recreated using two- and three-dimensional hydrodynamic modeling in a study by MacWilliams et al. (2006). The magnitudes from MacWilliam's two- and three-dimensionally modeled flow velocities are similar to those reported by Keller's one-dimensional model. Additionally, bulk velocity reversals as well as near-bed velocity reversals are apparent in MacWilliams' model results. However, the additional lateral component of the two-dimensional model predicts that the largest velocities in a lateral cross section occur over the point bar instead of the pool due to flow convergence at the pool head. Additionally, flow diverges between the tail of the pool and the head of the riffle, causing a lateral expansion of the sediment pathway as well as deposition on the riffle. Upstream and downstream of the riffle, sediment transport is concentrated in a laterally narrow zone. The three-dimensional model highlights a secondary circulation cell that may be responsible for fine material transport through the pool. As a result, MacWilliams et al. (2006) introduced the flow convergence theory as the key mechanism behind pool-riffle maintenance.

2.3 Sediment Routing Theory

Amongst several others disputing Keller's velocity reversal theory as an explanation for sediment routing through pools, Milan (2013) instead proposes that large particles travel around pools across point bars or around bar edges. Although certain flow structures such as eddies, reversals, or vortices, exist in the channel, their effect on sediment transport depends on their location. More specifically, despite the presence of a velocity reversal in the tail of the pool, Milan explains that it may not be the driving mechanism behind pool-riffle maintenance, as the reversal does not exist in an active zone of sediment transport. However, Milan's theory does not discount the existence of a velocity reversal, but states that it is unlikely to be the driving force behind pool-riffle maintenance. He provides a conceptual model comparing Keller's velocity reversal theory (1971) and a revised sediment routing theory, shown below in Figure 3. While studying a sinuous gravel-bed stream using tagged particles and bedload traps, Milan found that no sediment was transported into pools along the thalweg of the channel, as suggested by Keller (1971). In addition to the field study, computational fluid dynamics (CFD) performed on the pool-riffle unit confirmed these observations, showing that the trajectory of the flow's velocity steers away from the thalweg and overtop of the bar. The results from this study strongly indicate that the underlying mechanism behind pool-riffle maintenance is mostly sediment routing, and not velocity reversals. As noted in the MacWilliam's paper, changes in tractive force and the velocity reversal theory may nonetheless play a role in the removal of sediment that slides down the point bar face and into the pool (Milan, 2013). Milan's paper includes a graphic, shown below in Figure 3, depicting the differences between Keller's velocity reversal theory and Milan's revised sediment routing theory. Here one can see the differences between the two theories, most notable in the 90-100% bankfull figures (*d* in the Figure 3), where sediment travels through the pools in Keller's theory and overtop of bars in Milan's theory. Milan's schematic also depicts sediment travelling along the toe of bars, a phenomenon not included in Keller's theory.

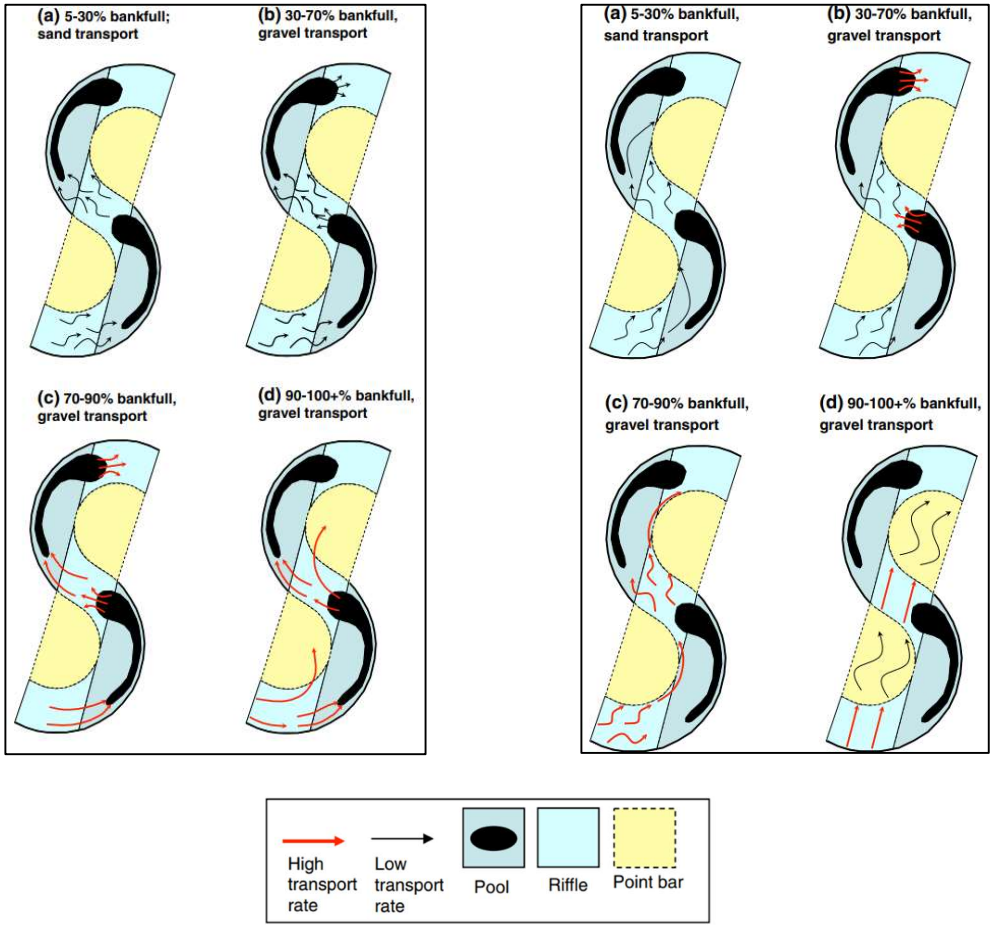

Figure 3. Sediment routing theory, left (Milan, 2013) vs. velocity reversal theory, right (Keller, 1971)

In a study researching a river bend with a frequently inundated floodplain in the Yuba River, California, White et al. (2010) investigate whether variable channel width causes a degree of flow convergence capable of maintaining a pool-riffle geomorphology. Using eight historical sets of aerial imagery coupled with digital elevation models (DEMs) from 1999 and 2006, a timeline of the channel's geomorphological evolution was created. Over the 22-year study, the river's planform significantly changed lateral and vertical position as a result of frequent floodplain inundation. However, eight notably persistent riffle crests were observed to remain in the same position throughout the study period. The riffles' persistence was observed to extend many years into history, as they were evident in aerial images from as far back as 1937. According to White et al., the most obvious similarity between the persistent riffles was the channel width, leading to the conclusion that flow convergence routing is responsible for increased sediment deposition due to lower velocities.

Another study investigating the Yuba River (Sawyer et al., 2010) used numerical modeling and field investigations to establish the effects of storm events on pool-riffle morphology. By measuring elevations in cross sections before and after the storm it was established that pool-riffle increased by 0.42 due to the higher discharge. Channel non-uniformity and evidence of variable flow-regimes support MacWilliams et al.'s theory of flow convergence routing (2006) as being the underlying mechanism of maintenance. During analysis, results from the two-dimensional model were compared to those from a numerical model, and it was established that the two-dimensional model failed to accurately portray localized channel change across cross-sections due to subscale variability of the bed.

Compared to Milan (2013), MacWilliams et al. (2006), and Papangelakis et al. (2020), Clayton & Pitlick (2007) provide an alternative sediment routing theory and discuss fractional bedload transport in river bends. The former studies hypothesize that sediment is routed towards the inner bank. As discussed by Milan (2013), the larger the discharge becomes, the more water is routed across the bar, effectively transporting larger sediment classes than at smaller flows. Contrarily, Clayton & Pitlick postulate that larger particles will be steered towards the outer bank of the bend due to greater shear stresses in this region, although it should be mentioned that the latter study assumes a more frequent, lower flow than discussed in Milan's study. In addition to bed load samples, sediment samples were taken at the surface and the subsurface. The largest rock was identified, measured, and plotted against lateral distance. Although there was a slight positive correlation between distance towards the outer bank and particle size, the relationship is weak ($R^2 = 0.21$), indicating that there is a need for more controlled studies to fully describe and understand the phenomena.

In a 2020 field study on Wilket Creek investigating the effectiveness of pool-riffle restoration, the movement of large clasts was tracked during storms events (Papangelakis et al., 2020). The experiments were performed on three separate river reaches: a rural reach, an unrestored urban reach, and a restored urban reach. The two urban reaches are in Toronto's Wilket Creek –the creek studied in this paper– while the rural reaches are in Pickering's Ganatsekaigon Creek. Amongst several other measurements, large clasts equipped with radio frequency identification (RFID) tags were placed in the river and tracked over several years. The tracked clasts, or tracers, were selected to represent the D_{50}, D_{75}, and D_{90} size classes found in Wilket Creek, and were seeded across a riffle in the unrestored reach, and across two pool-riffle sequences as well as a point bar in the restored reach. In bends, which consist of a point bar along the inside and a pool along the outside of the channel, particles

exclusively moved across the point bar. In riffles upstream of pool-bar systems, tracers were found to approach the pool overtop of the riffle, especially evident in the larger storm event (lowest subfigure in Figure 4, $f_m = 0.53$). Once retrieved, several tracers were found on the tail of the point bar, upstream of the next riffle, insinuating that a mechanism was pushing them towards the inside bank of the channel. Almost no tracers were found in the actual pools studied, while several were deposited on the bar. The pathways of the tracers are shown in Figure 4 below, and show emphasize the tendency of large particles avoiding pools during storm events, and instead depositing on riffles and point bars.

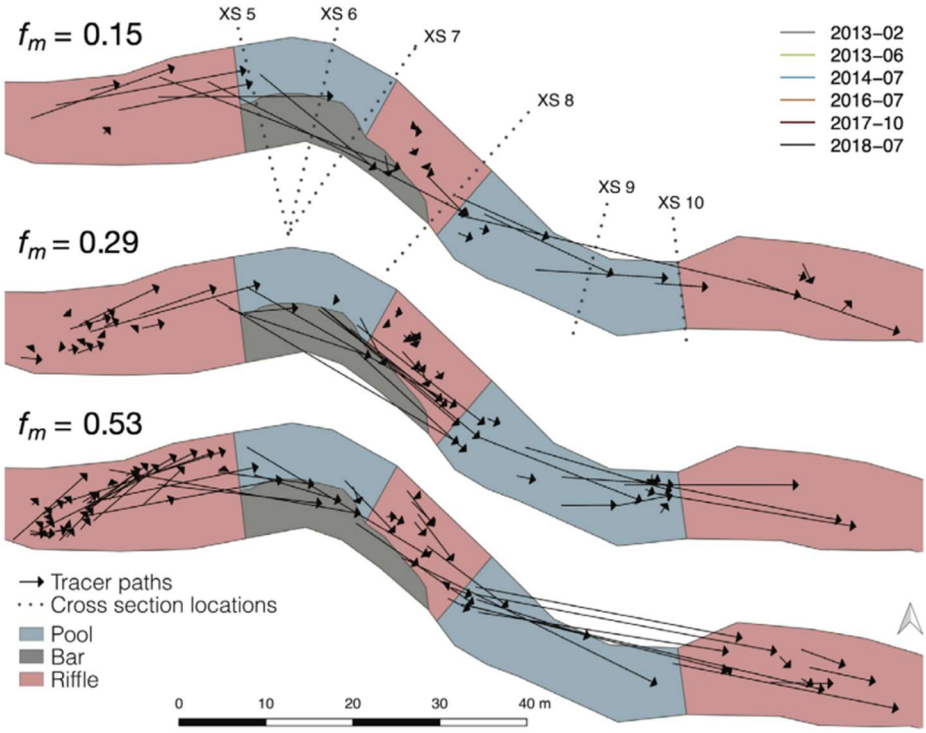

Figure 4. Tracer pathways deflecting over bar (Papangelakis & MacVicar, 2020)

2.4 Lab Experimentation on Riffle-Pool Systems

In addition to field experiments performed on Wilket Creek, several lab-scale flume studies were conducted on the creek with the specific goal of studying sediment routing patterns in meandering channels.

In addition to the lab experiments that investigate sediment routing in Wilket Creek specifically, other laboratory studies have been performed with the goals of investigating the effects of variable geometry, different types of reversals, sediment thickness, and unsteady sediment supply on pool-riffle maintenance in other watercourses. Each of these studies add insight to how rivers function naturally and continue to bridge the gap between physical river models and real-world observations.

In Chartrand et al. (2018), a pool-riffle system was investigated using an unsteadily flowing, sediment fed physical experiment, with a goal in studying the effect of variable width on channel slope, and therefore the emergence of pool-riffle systems. Beginning with a bed full of sediment, experiments depicted that riffles were found to form in wide reaches, while pools formed in narrow reaches. In areas where width was constrained, a coarsening of bed material was observed. These results persisted during all experiments performed, which employed a wide range of flows and sediment rates. Additionally, the experimental results agreed with their mathematical model, which relates local slope (S_{local}) to the ratio of flow and time of particle entrainment (Λ), and dimensionless velocity (ΔU^*_x), which considers differences in lateral velocity as well as depth. Two main types of pool-riffle systems were defined: entrainment driven and depositional driven systems. The mechanisms behind these two types of pool riffle systems were found to occur in different conditions, as entrainment-driven systems occurred upstream of narrowing reaches, while depositional-driven systems occurred upstream of widening reaches. This idea is an important observation in the scope of flow divergence and flow convergence, linking sediment transport observations to hydraulic observations. Chartrand et al. notes that several facets involving physical experimentation on pool-riffle systems remain unstudied, and that the consideration of local turbulence in the channel could provide additional, important insight into governing mechanisms.

Recognizing that the velocity reversal theory cannot independently explain self maintenance in pool-riffle systems, Bayat et al. (2017) investigated the impact that more complex mechanisms may have on the system as a whole; namely multidimensional flow patterns and multifractional sediment transport. These mechanisms were observed in a physical recreation of Bear Creek, located in Arkansas, USA. Two steady, discharges representing an intermediate and a high flow were run through the flume, during which three-dimensional velocity distributions were observed at five locations throughout a given pool-riffle couplet. Results from the study indicate that complete velocity reversals, as described by Keller (1971), are not required to maintain pool-riffle patterns in rivers. As similarly posited by MacVicar et al. (2010) in their critique of the Caamaño criterion

(Caamaño et al., 2009), flows as low as $1/7^{th}$ of bankfull discharge create local sediment transport reversals, sufficient in maintaining said pool-riffle patterns. When comparing two pool-riffle couplets, it was determined that complete velocity reversals were more relevant in couplets where the pool was straighter and more laterally constricted, as seen by more uniform grain size distributions between the couplet's pool and riffle.

Hassan et al. (2021) expanded on the experiments performed by Chartrand et al. (2018) by investigating the impact on a single pool-riffle system in the case of an upstream change in sediment supply. The basis for analysis was based off methods described in Chartrand et al. and added to in the way of a more rigorous statistical analysis of pool-riffle behaviour. Experiments were performed under various flow and sediment feed conditions. Half of the experiments were unfed, while the other half were fed with various sediment feed rates. Similar to Chartrand et al., results indicated that channel width was the driving factor behind pool and riffle position. By observing the sediment thicknesses in pools and riffles over several flood conditions, it was noted that, during high flow, sediment in pools decreased in thickness faster than in riffles, a result that agrees with Keller's velocity reversal theory (1971). However, more localized measurement resulted in a less clear, or in some cases, non-existent reversal in velocity, suggesting that local system response depends on many variables. Results from the evolution of grain-size distributions in pools and riffles over time indicate that the bed continues to rearrange itself even after equilibrium is reached. Both Hassan et al. (2021) and Bayat et al. (2017) identify clear research gaps related to physical models of meandering rivers.

Another study researching the importance of variable width and unsteady flow for pool-riffle maintenance using a physical model was performed by Vahidi et al. (2020). A series of symmetrical hydrographs modelled after 1-, 2-, and 3-year storms in Bear Creek, California, were directed through two identical pool-riffle couplets. Three main hypotheses were presented before experimentation: 1 – flow changes due to channel width variations are the driving mechanism behind pool-riffle maintenance; 2 – self-maintenance processes are sufficient for rapidly restoring the system to an equilibrium state; and 3 – self-maintenance processes are insufficient in restoring the system to an equilibrium state in the span of one flood but may be enough over many floods in sequence. Several notable results pertaining to the legitimacy of these hypotheses were observed. The narrow centre of the pool never filled in completely, confirming Vahidi et al.'s first hypothesis. However, since pool-riffle self-maintenance was not accomplished during any of the experiments, it can be inferred that shear stress, velocity, or transport reversals are not sufficient for complete pool-riffle maintenance,

causing Vahidi et al. to reject the second hypothesis. When comparing shorter hydrographs to longer hydrographs, it was determined that longer experiments resulted in greater sediment buildup over riffles, while shorter experiments did not complete the same difference in pool-riffle elevation, indicating that the third hypothesis was satisfied. Vahidi et al.'s concluding remarks notably mention that meander-induced secondary flow does not play a large role in pool-riffle maintenance, based off a previous study which replicated the channel's geomorphology using a 1-D model.

In experiments performed by Bankert and Nelson (2017), a scaled down model's bed at steady state was observed while undergoing increases and decreases in sediment supply. Development of bedforms was monitored by draining the flume between experiments before taking pictures, which were later transformed into digital elevation models using 'structure from motion'. In addition to the pictures, subsurface stratigraphy samples were taken from various bar and pool locations throughout the flume. During the initial bedform formation, beginning at an empty bed, the material making up the bars was relatively coarse. After the feed rate was increased initially, the bars grew laterally, mainly due to the build up of fine material, and was topped with coarse material at the highest point of the bars. After the second increase in feed rate, lateral aggradation increased to an extent where pools were filled in, and an intensification of shear stress occurred along bar edges, causing lateral erosion of stable bars. At the end of these experiments, slight migration of bars in the downstream direction was noted. During the degradation experiments, the fine material was stripped away, revealing the coarser pre-aggradation material. This latter observation, if proven to exist in real-world channels, would suggest that coarse material is imperative for structurally sound bedforms, creating an armour layer that locks down fine material.

In a later, similar study performed by Morgan and Nelson (2021), different channel configurations were subjected to three different types of experiments: steady flow with a steady sediment feed rate, unsteady flow with a steady feed rate, and unsteady flow with a doubled feed rate. The first channel configuration was straight with straight channel walls, while the second channel was straight with sinusoidal walls. Apart from the different channel widths, all other variables were kept the same while performing experiments in both configurations, allowing for the identification of different mechanisms. Specifically, it was hypothesized that, in the variable width channel, the bedform response to unsteady flow would display greater sorting between pools and riffles when compared to the constant width channel. Results from the experiments showed a minimal response to the introduction of unsteady hydrographs in both channel configurations. The two channels adjusted to

the increased sediment supply in different ways; the constant-width channel experienced a steepening effect, while the variable-width channel decreased bar-pool relief and riffle-pool relief as bars grew laterally and pools filled in. These results indicate that high flow events may be responsible for pool-riffle maintenance, causing greater heterogeneity between pools and riffles. Morgan and Nelson identify several research gaps in response to the experimental findings of this study, including how grain size sorting plays a role in pool-riffle formation, whether smaller grain size classes could be responsible for the mobilization of coarser particles, and how alluvial floodplains and channel banks would respond to an increase in sediment supply.

With respect to their methodologies and results, laboratory experiments performed by Peirce et al. (2021) were similar to the experiments performed in the field by Papangelakis et al. (2020). A model mirroring Wilket Creek's planform was set up in a flume located at the University of Waterloo. In the study's experiments, the sediment supply rate was altered to investigate the alluvial cover response, while keeping the flow through the channel steady. The results from these experiments show that increases in sediment feed rate result in more pronounced bar-connecting features. Although equilibrium was not achieved for all particle sizes, the sediment output trends indicate that fine sediment was largely stored in bars, while coarser particles were less likely to find a stable spot in the channel. The particle path was found to remain along the toe of the bars, instead of detaching from the path and impacting the outside wall or traveling into the outer pools. Peirce et. al. (2021) also uses hypsometric curves to present results from the performed experiments. These curves, which compare relative depth to relative covered area in the flume, indicate that an increase in feed rate results in a greater variability in cover depths. Additionally, further analysis of the hypsometric curves show that sediment starvation leads to the flattening of the hypsometric curve's slope, indicating a greater invariability between depths in the channel.

In Papangelakis et al. (2020), alluvial cover dynamics in a regularly shaped sinusoidal channel were investigated. The channel morphology was built up from a bare bed by running water through the flume while simultaneously feeding sediment at the upstream end of the flume. The first bars to form in the flume were 'proto bars', or pockets of sediment that form on the inside of bends, slightly upstream of the bend's apex. Once the bars grew to fill the bend, they would begin to connect via 'diagonal, riffle-like structures', which were made of coarser material than the bars. Sections between bars and along the outside of bends were observed to remain bare, a pattern that persisted with

increases in sediment feed rate. Sediment flow was found to preferentially travel along the toe of bars and along the riffle between bars, avoiding the outsides of bends.

A gap in research with respect to particle transport pathways existed in both methodologies implemented in Peirce et al. (2021) and Papangelakis et al. (2020). Only visual observations concerning sediment routing were performed, and most deductions involving sediment transport revolved around erosion and deposition. Results regarding individual particle location and pathways have historically been very difficult to attain, although this information would provide important insight into pool-riffle maintenance, bedform construction and destruction, and fractional bedload transport. Understanding the different roles that particles in different locations and grain size classes play would provide valuable information for river restoration practitioners and could aid in the development of new restoration techniques and practices. Additionally, experiments from the two previous studies were only performed under steady flow, and sediment transport patterns change significantly with flow (Lisle, 1982; Wilcock et al., 1996). By including experiments where flow increases, peaks, and decreases in a similar manner to real-life storms, a more realistic channel response can be obtained. In turn, these insights will enable engineers to better equip natural channel designs to handle a range of flows.

Chapter 3 Methodology

3.1 Creek Model

In order to investigate spatial and temporal patterns in a river, several laboratory experiments were performed on a physical model. The experiments were run in a 1 to 40 scale physical model of Wilket Creek, used initially by Peirce et al. (2021) to investigate sediment cover dynamics over a partially alluvial bed. The physical model, deployed in a 13.3-metre-long, 2-metre-wide flume managed by the University of Waterloo, is a reproduction of an unrestored reach of the creek. In 2015, a survey of the thalweg and the top of banks was performed on the reach of interest, allowing for the irregularly meandering planform to be scaled down and carved into foam blocks (Peirce, 2021). The topography of the banks and bed were not reproduced to limit the complexity of construction. Instead, the creek was represented as a simple trapezoidal channel with a flat bed, the banks angled at 30º from the vertical. Two duplicates of the model reach were placed in series to one another to allow for duplication of results and to limit the influence of the upstream and downstream boundary conditions. The roughness characteristics of the smooth underlying clay till in Wilket Creek was reproduced by lining the channel with sand grains, affixed using glue. Finally, the channel was painted light blue as a way of creating contrast between the sediment and the bed. An image of the model is shown in Figure 5 below.

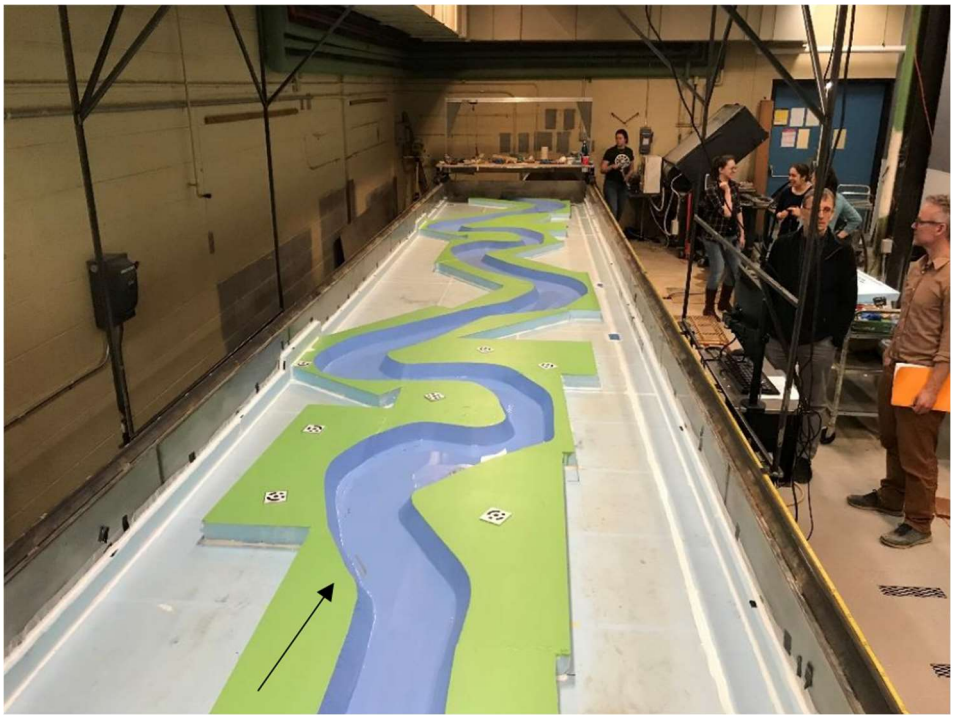

Figure 5. The physical model of Wilket Creek in the flume.

Water flowing into the flume was controlled by an ASCO air pressurized valve, which can be preprogrammed to recreate hydrographs from a simple time series using the software LabVIEW. Water flowed into a head tank and passed over a sharp-crested triangular weir before entering the channel. A relationship between the height above the weir and flow (shown below) was established as per Pospíšilík & Zachoval (2023), allowing for visual confirmation of the flow, where y is the depth of water above the 90-degree notch in metres, C_d is the discharge coefficient (242, as per Peirce et al., (2021)), θ is the degree of the notch, g is gravity, and Q is flow in litres per second.

$$Q = \frac{8}{15} C_d \tan\left(\frac{\theta}{2}\right) \sqrt{2g} y^{2.5}$$

The flow chosen for the experiments was based off Peirce et al.'s (2021) study using this model, as well as Welber et. al. (2020). A hydrologic study of the watershed (AECOM, 2011) found a 2-year design flow through the creek to be approximately 19.5 m^3/s. Using Froude scaling, a method outlined by Julien (2002) and Frostick et al. (2011), the design flow was appropriately scaled down to an experimental discharge. Froude scaling partly involves converting the length scaling factor Z_r of the model (40 in this study) into flow and time scaling factors Q_r and T_r which were found to be

10100 and 6.32 respectively. In the model, this results in a flow 10100 times smaller than the unscaled flow and a storm 6.32 times shorter than the unscaled design storm. Scaling the model parameters in this way ensures that the relative roughness, dimensionless shear stress, and storm duration from the original, real-world channel is mirrored in the laboratory model (Julien, 2002).

3.2 Measurements

Three main measurements were made during experimentation. Sediment import and export was measured using the basket system at the downstream extent, allowing for storage monitoring. DEMs of the bed's topography were created using two cameras and the structure-from-motion software, Agisoft. Finally, individual sediment particle pathways were extracted from UV-lit video recordings processed in the tracking software TracTrac.

3.2.1 Sediment Import and Export

The size distribution of the sediment mixture used in these experiments was the same as the distribution used in Peirce et al. (2021). The mixture was geometrically scaled to reflect the particle sizes in Wilket Creek, which was a poorly sorted mixture of sand and gravel derived by Bevan et al., (2018). The distribution is shown in Table 1 below. Particles painted with UV-sensitive paint were included in the mixture, where orange, green, and pink particles were sized to represent D_{60} to D_{85} (1.18 – 2.36 mm), D_{85} to D_{99} (2.36 – 4 mm), and larger than D_{99} (4 – 5.6 mm) size classes respectively. Only 5%, 12.5%, and 25% of small, medium, and large particles respectively were painted as to avoid overcrowding the region of interest, which would make it difficult for the particle tracking software to distinguish between particles.

Table 1. Sediment Supply Grain Size Distribution

Grain Size Class (mm)	Fraction (%)
4 – 5.6	1.8
2.36 – 4	12.1
1.18 – 2.36	25.7
0.6 – 1.18	29.5
0.3 – 0.6	21.9
Pan – 0.3	9.0

A sediment hopper equipped with a horizontal screw auger uniformly pushed the sediment mixture into the most upstream part of the channel, while ensuring that the sediment remains mixed. The dial reading was set based on a rating curve (Peirce et al., 2021), confirmed prior to each experiment. Using a half-pipe, the sediment was routed from the sediment hopper outlet into the upstream part of the channel.

At the downstream end, the effluent mixture of water and sediment flowed out of the downstream end of the flume, and into mesh-lined baskets. Baskets were exchanged at regular time intervals by attaching the basket to a gantry equipped with a pulley system, pulling the basket away from the flume outlet, and placing an empty basket in its place. The pulley system was equipped with a digital scale, allowing for the sediment sample to be weighed. After removing the basket from the outlet, it was left to drain for two minutes. After two minutes, the gravel and sand mixture will have reached field capacity. At this time, the weight was recorded, and the basket's contents were emptied into a bag. The empty basket was reattached to the pully system, and the weight was recorded. After all sediment samples were collected, they were dried in an oven and weighed once again. A grain size distribution was created for each sample by feeding the sediment through a stack of 10 sieves. The mesh sizes for the sieves were 5.60, 4.00, 2.80, 2.36, 1.18, 1.00, 0.71, 0.60, 0.50, and 0.30 millimetres. Sediment falling through the 0.30 mm sieve was caught in a pan. A waning sediment sample, meant to capture any sediment mobile during the drawdown, was retrieved from the mesh baskets. These samples were found to be much smaller than the previous sample, and contained less than 5% of a typical sample's mass. Due to the length of the drawdown effect with respect to the experiment's duration, it is believed that the DEMs still provide important insight to the mechanisms active in the channel.

A diagram of the apparatus is displayed below in Figure 6.

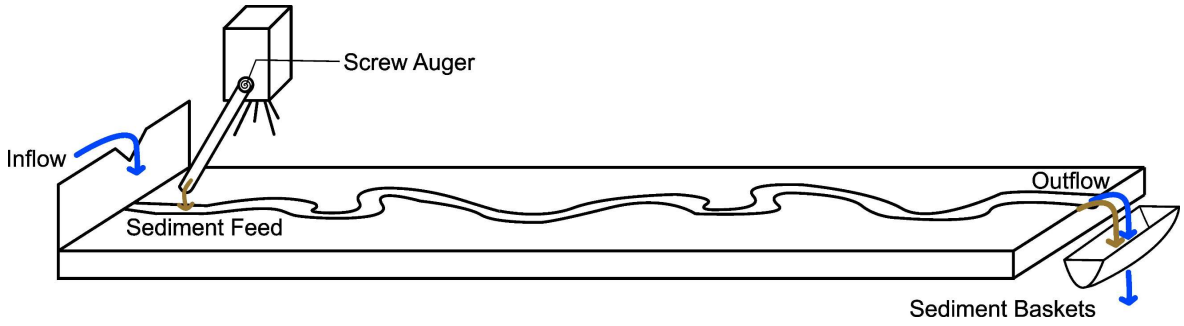

Figure 6. Diagram of apparatus, displaying inflow, sediment feed, and downstream baskets

The effect of biological fouling on the substrate was considered, as the same sediment mixture was used throughout the eight months of experimentation. The formation of biofilms, as well as other types of sediment fouling have been observed to change the sediment transport characteristics in a river. In a flume study on the bed stability of cohesive material in a wildfire affected stream, the resistivity of sediment to erosion was observed to increase with the formation of biofilms (Stone et al., 2011). Thus, the sediment in the channel, as well as the effluent and recycled influent sediment, was visually and olfactorily monitored to ensure that no biofilm had formed. The presence of a biofilm in the channel may have resulted in a gradual decrease in global aggradation, a phenomenon which was not observed.

3.2.2 Topographic Analysis

After the experiments were completed and the bed was left to dry, two Canon EOS Rebel T5i cameras were used to capture several images of the bed, once again using the sliding cage. The images were captured with a focal length of 20 mm at a resolution of 5184 x 3456 pixels, resulting in a 0.53 mm per pixel ratio. Capturing the bed from both the left and right sides of the channel allowed for the creation of a stereoscopic image, or an image with an added topographical element. As per the methods used in previous studies employing the use of Structure-from-Motion (Morgan, 2017; Leduc, 2019), the photos taken along the length of the bed were stitched together using Agisoft Photoscan 1.4, an operation requiring the placement of several control targets. Relative coordinates of these control targets were programmed into the Agisoft script. The resulting digital elevation models and orthomosaic images were exported at an areal resolution of 1 mm and a vertical accuracy of 2.4 mm +/- 0.6 mm. The accuracy was established by comparing the known benchmark coordinates with the elevations calculated by the Structure-from-Motion operation. Due to instrumental limitations, the flume must be drained before pictures used to create the DEMs are captured. During the draining process, a drawdown effect was observed to alter the bed slightly.

A large cage, equipped with halogen lights, UV-lights, and cameras slides along the length of the flume. The unique lighting setup allows for precise particle movement observation. The three painted size classes, which partially make up the influent sediment mixture, were painted with UV-sensitive paint. A Panasonic-DC-BGH1 camera, filming 60 frames per second at a resolution of 1080 by 1920 pixels, was mounted to the frame and trained onto the region of interest. The region of interest was covered with a black sheet to avoid light pollution, allowing for consistent lighting conditions

between experiments. The camera was controlled remotely using the Lumix Tether for Multicam application. The recorded experiments, illuminated by the UV-lights, clearly show the movement of individual orange, green, or pink particles, as well as the evolution of bedforms consisting of fine material. The UV-lights were set up behind the camera to reduce the amount of surficial reflection. During the three-hour equilibrium experiments, thirty second clips of the ROI were filmed. The shorter storm and reset experiments were filmed in their entirety. A key showing the observed ROIs is shown in Figure 7 alongside Table 2 showing the regions filmed in each experiment.

Table 2. Regions Filmed in Each Experiment.

Region of Interest	Experiments
1	Alternating Experiments 5 – 8, Degradation Experiments
2	Alternating Experiments 3 – 4
3	Equilibrium Experiments 1 – 4, Alternating Experiments 1 – 2
4	Alternating Experiment 11 – 13
5	Alternating Experiment 9 – 10

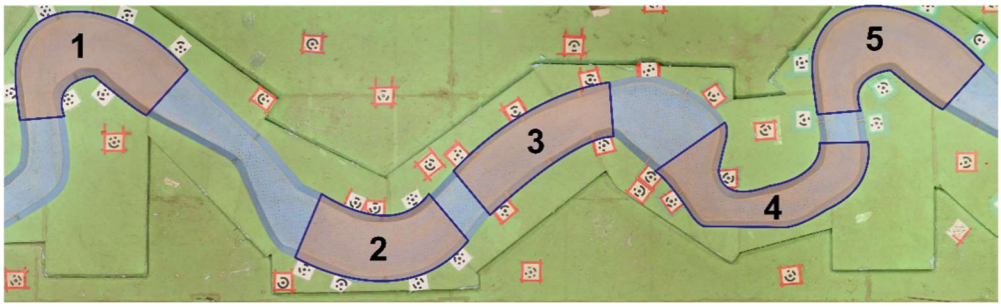

Figure 7. Key showing regions of interest filmed during particle tracking analysis.

3.2.3 Particle Tracking

The individual tracking of the orange, green, and pink tracers was made possible by extracting each colour class from the raw video recordings. This operation was performed using a custom MATLAB algorithm which allowed users to assign CIELAB (L*a*b*) colour space profiles for individual colour classes. The CIELAB colour space consists of three parameters: white / black, red / green, and blue / yellow. The addition of a new candidate tracer shifted the thresholds for each colour space parameter, effectively creating a unique colour profile for each tracer colour in a given lighting

condition. This operation was performed on each frame of the experimental videos, superimposing the particles in the size class of interest overtop a black background. These operations were repeated for each video due to the changes in lighting conditions and region of interest.

After the videos were masked for each colour class, they were loaded into TracTrac, a third-party open-source particle tracking software (Heyman, 2019). The software employs a Lagrangian, Particle Tracking Velocimetry (PTV) approach, where each tracer's trajectories is recorded between frames. Certain parameters in the TracTrac software can be adjusted to better capture the different tracer size classes. A table containing the parameters used for the different tracers is shown below. The resulting particle trajectories are saved as an ASCII file, where a given tracer's position is stored for each frame. Selection of parameters and general methodology surrounding particle tracking is expanded on in a methodological paper released parallel to this study (Iun et al., in preparation). The noise filtering size removes particles below a certain pixel quantity, while the blob scale defines the average size of each particle.

Table 3. TracTrac parameters used for each tracer type

Parameter	Orange	Green	Pink
Background Model	Off	Off	Off
Noise Filtering Size	1	2	3.5
Object Type		Bright	
Detector		Difference of Gaussians	
Blob Scale (px)	3	5	9
Peak Neighbours	1	3	4
Intensity Threshold		Auto	
Sub-pixel Method		None	
Motion Model		Unsteady	
Frames		3	
Iterations		3	
Filter Outliers		No	

3.3 Experiments

Over the span of approximately eight months, twenty-two experiments were performed in sequence to one another, and their order is shown in Figure 8. Parameters such as feed rate and flow varied between experiments, allowing for the analysis of multiple mechanisms, as well as comparisons between the current study and previous studies performed on the Wilket Creek model. Experiments were performed in sequence to one another, where the initial conditions of one experiment were the ending conditions of the previous run. At the beginning of each experiment, the pump was turned on and the correct input hydrograph was selected. As soon the initial surge of water flowed under the point where sediment was input into the flume, the sediment hopper was turned on. Depending on the experiment, a period of time passed until the mesh basket catching the sediment at the downstream end of the flume was removed from the flow and weighed using the basket weighing procedure described in Section 3.1. This was repeated until the flow was shut off, at which point one last basket was left to catch any sediment flowing out of the flume during the drawdown period. This sample was labelled as 'waning'.

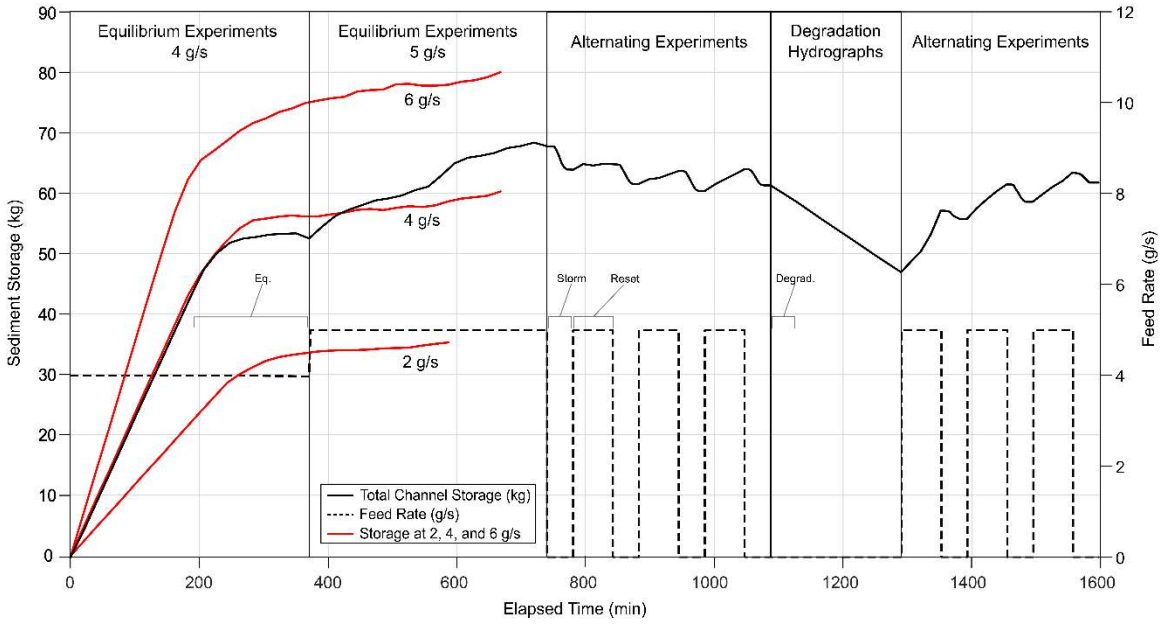

Figure 8 Experimental design, including experiment order, experiment feed rate, sediment storage, and comparisons from Peirce et al. (2021)

Experiments were split into three types: equilibrium experiments, alternating experiments, and degradational experiments. The two main objectives of the equilibrium experiments were to allow the flow to establish a naturally formed channel geomorphology, and to allow for comparisons to Peirce et al.'s (2021) similar experiments. All equilibrium experiments were performed at a constant flow rate of 1.9 L/s to match the flow rate in Peirce et al. (2021). The first two of four equilibrium experiments were performed with a feed rate of 4 g/s, while the feed rate for the third and fourth equilibrium experiment was increased to 5 g/s. Baskets were emptied every 20 minutes, resulting in 10 sediment samples, including the waning sample.

Alternating experiments consisted of a 35-minute-long, unfed, triangular hydrograph, followed by a 60-minute-long, fed, constantly flowing experiment. The unfed hydrographs were referred to as 'storms', while the fed, constantly flowing experiments were referred to as 'resets'. The goal of these experiments was to investigate the effects of sediment-starved, unsteady flow on an equilibrium-state pool-riffle morphology, while ensuring that the constantly flowing experiments returned the bed back to a state of equilibrium. The storms consisted of five minutes of a 0.35 L/s baseflow, a gradual increase to a peak flow of 2.16 L/s, a gradual decrease returning to 0.35 L/s, and another five minutes at this baseflow. The sediment baskets were emptied at regular intervals, resulting in ten sediment samples, including the waning sample. The resets consisted of a constant flow of 1.9 L/s, during which the baskets were emptied every 15 minutes. Both types of experiments were filmed in their entirety. Although 13 alternating experiments were performed in total, consisting of seven unfed, triangular hydrographs and six constantly flowing experiments, the alternating experiments were performed in 2 batches, which were separated by a set of degradational experiments.

The degradational experiments were performed after four unfed, triangular hydrographs and three fed, constantly flowing run. The experiments consisted of five unfed, triangular hydrographs, and were run with the goal of investigating the geomorphology of the bed during a longer period of sediment starvation. Consequently, the remaining experiments were run on the sub-equilibrium state bed.

During each experiment, the effluent sediment mass was subtracted from the influent sediment to attain the storage in the flume. The stored mass is shown is Figure 8, calculated as the mass added to the flume minus the mass that was exported and caught in the baskets. Mass accumulation curves from Peirce et al. (2021) are also shown for comparison. Results of the sediment mass balance are presented in more detail in Section 4.1.

Chapter 4 Results

4.1 Sediment Import and Export

Storage in the flume increased rapidly during the first 200 minutes before plateauing at approximately 53 kg. This period coincided with the first significant interval where sediment was exported from the flume, indicating that the storage relationship initially follows the pattern of a breakthrough curve.

A similar analysis was performed by Peirce et. al. (2021), allowing for a comparison between experiments. This initial mass rate of 4 g/s was chosen to replicate one of the three mass rates used in Peirce's experiments. As seen in the storage relationship comparison, the initial rate of aggradation in the two sets of experiments where the feed rate was 4 g/s match each other very closely, although equilibrium is established earlier and at a lower storage in the current study's experiments. Even though the results from the two studies are not identical, patterns observed in Peirce et al.'s experiments are confirmed during the current study, as equilibrium is reached after the 6 g/s experiment and before the 2 g/s experiment. After the initial rapid storage increase in both experiments, the rate of aggradation slows in both sets of experiments. In the current study, the end of the 4 g/s feed rate is accompanied by a slight dip in storage, which coincides with the termination of the pump, and a drawdown in water level throughout the channel. Analyzing the small discrepancies between the two studies' results aids in analyzing the effects of small methodological differences. For example, in Peirce et al., the topographic analysis was performed at a greater frequency than in this study, resulting in a greater frequency of flow cessation. This difference may not have been important enough to cause large differences in the results but may be the reason for the lower equilibrium storage in this study.

After the four initial, 180-minute-long experiments were performed, a series of alternating experiments were run over the naturally formed geomorphology. The alternating experiments began at the storage level established at the end of the 5 g/s fed equilibrium experiment. During the unfed storms, the storage level in the channel quickly decreased. Although the channel storage was different at the starting points for each storm, the rates of storage decrease were relatively similar to each other. The anomaly to this observation was storm #5, the first storm performed after the degradation experiments. Instead of dropping 4 kg, as observed in the other storm experiments, the storage during storm #5 only dropped approximately 2 kg, before plateauing at 56 kg.

During the fed resets, the channel storage increased proportionally to the initial storage condition. The first reset, which had the highest initial storage, was performed shortly after equilibrium was established in the initial set of experiments. During this experiment the storage remained constant, implying that the mass of imported sediment matched the mass of exported sediment. As the initial storage levels for the following reset experiments decreased, a clear trend can be observed: the lower the initial storage level, the greater the rate of aggradation will be in the following reset experiment. The most notable example of this phenomenon occurs during reset #4, the experiment following the degradation experiments.

The degradation experiments performed after the first seven alternating experiments provide insight into the effects of long-term sediment starvation. During the five unfed storms, the channel storage linearly decreased until the end of the last experiment. The final storage level settled at approximately 47 kg, lower than the 4 g/s equilibrium level established in the equilibrium experiments.

A grain size analysis was performed on the dry samples by sieving the samples into size fractions. This analysis shows that the size distribution of the exported sediment varies in response to flow regimes and bed condition (Figure 9). Fine material and coarse material are shown on the left and right ends of the graph respectively. Export during unfed experiments was compared against a hypothetical feed rate of 5 g/s. Experiments are presented in chronological order, beginning with the equilibrium experiments. The alternating experiments are split into those performed before the degradational experiments and those after. Two figures for each set of alternating experiments are provided: one for the fed, constantly flowing reset experiments, and one for the unfed hydrograph experiments. This breakdown allows for comparison between similar experiment types, although it should be noted that the similar experiments were not performed in sequence (except for the degradation experiments). As for the storage level comparisons, the export fractions are compared against experiments performed by Peirce et al. (2021), depicted as a black dotted line in all figures. The export fractions from Peirce et al. were measured during the last 5 intervals of the equilibrium experiment, which were assumed to represent the steady-state condition of the bed.

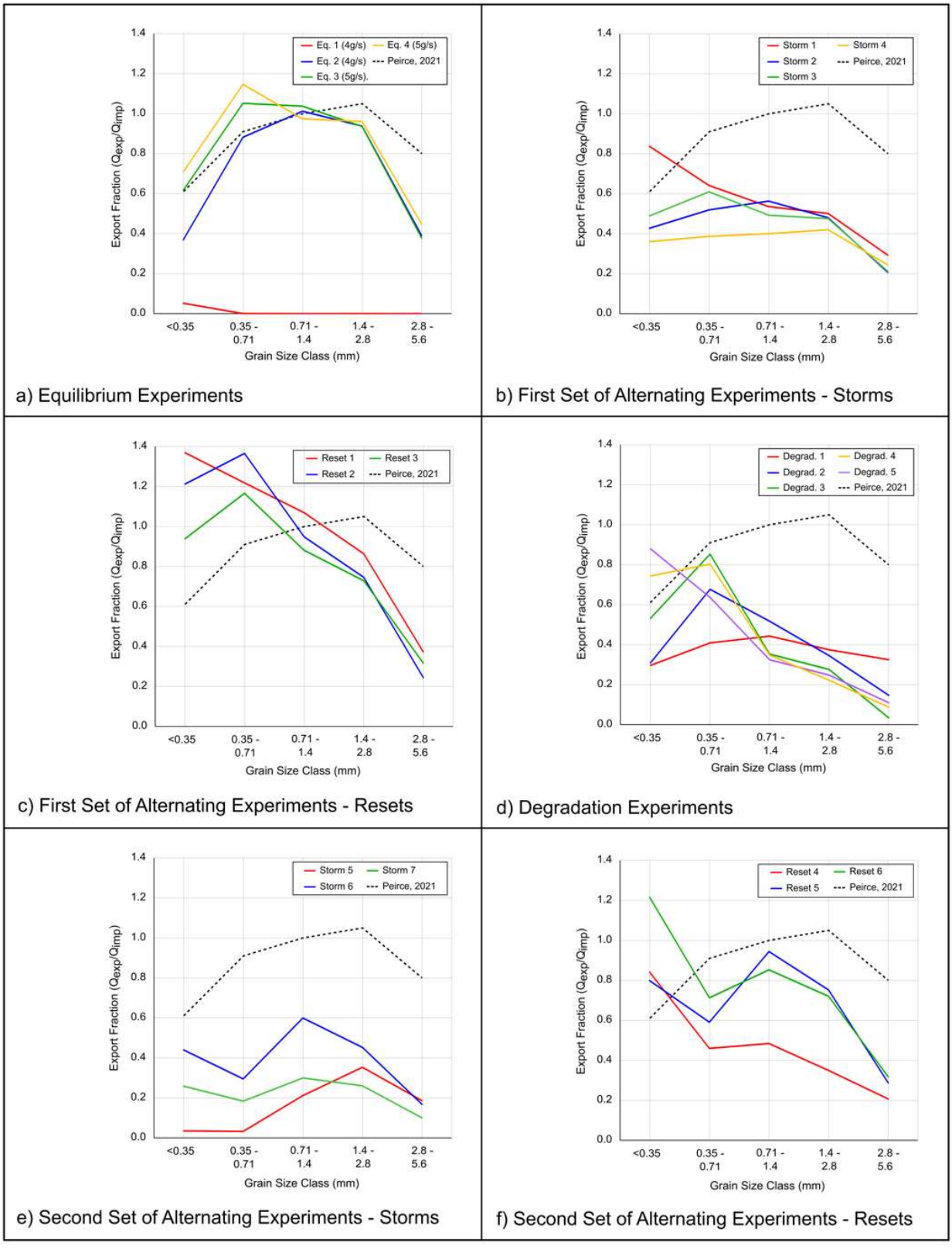

Figure 9. Export fractions for each experiment type, depicting the relative sediment export for each grain size

As seen in Figure 9a, during the initial equilibrium experiment the imported sediment had not travelled through the flume, and as shown in the previous storage experiments, breakthrough had not yet occurred. Although no significant amount of export was recorded in any size class, a small amount of fine material – on the order of 5% of the imported fine material – was exported during the initial experiment. Generally, the shape of the export fraction relationships developed during the equilibrium experiments were similar to the expected results, presented by Peirce et al. (2021). The export fractions are close to one for the middle sizes and less than one for the small and large particle sizes. Some small differences were noted in in the coarse fractions, as results from Peirce et al. (2021) generally showed a larger export than this study. Both studies displayed a disproportionate retention of both coarse and fine material, while medium-sized material was exported at approximately the same rate as was imported. In this study, the amount of exported fine material increased slightly as time passed and as the feed rate increased, indicating that less fine material was being stored in the flume as the channel reached equilibrium. In the final equilibrium experiment, the export fraction of fine material increased, while the export fraction of medium material decreased. The export fractions for coarser material did not respond as the storage approached equilibrium, or as the feed rate was increased. Analyzing the size of exported material during the equilibrium experiments aids in determining which grain sizes were used in the initial construction of bedforms in the channel. A lower export fraction of a given grain size would indicate that this particle class was retained in the channel and used for construction.

During the first set of alternating experiments, shown in Figure 9b and 9c, distinct differences between the storm and reset experiments' export fractions were observed, and more notably, between similarly fed reset and equilibrium experiments. When sediment-laden flow was routed over a mature bed during the reset experiments, a disproportionate amount of fine material was exported (90 – 140% of imported material), while the coarse export fractions remained low. Comparatively, when sediment was fed into an empty channel during the previously performed equilibrium experiments, much more fine material remained in the channel. The sole difference between the fed reset experiments, and the equilibrium experiments performed in this study and in the study by Peirce et al. (2021), is initial storage. While the equilibrium experiments were performed from an empty bed, sediment-laden flow was routed over a developed bed during the fed reset experiments, implying that while fine material may be used for initial bar construction, it was not deposited over mature bars. During the unfed storm experiments, sediment exported in all size classes was between 20 – 40% of the imported sediment, as most of the material was retained within the channel, with the exception of

the first experiment where 60% of imported sediment was exported. As the overall storage in the channel decreased during the first set of alternating experiments, the export fraction relationships became progressively flatter as more material was being used for bar reconstruction. Medium size classes underwent more export than during the unfed storms. The declining trend in overall storage coincided with a decrease in fine export, while the coarse export fraction remained relatively constant. Understanding how sediment transport changes as a river matures can provide significant guidance for restorative design. Usually, restoration projects focus on mature rivers, and observations from the alternating experiments may be more relevant than those from the equilibrium experiments.

Five degradation experiments, displayed in Figure 9d, were performed after the first set of alternating experiments. The first experiment out of five resulted in a well graded sediment export. However, as the bed experienced more erosion, an increase in fine material export and a decrease in coarse material export was observed. In both the first degradation experiment as well as the previous storm experiments, the channel's storage was in a state of equilibrium. A strong, size-dependant transport relationship was observed in the sediment export as the channel storage dropped below equilibrium storage. In contrary to the fine material, the coarse material export was much less variable. No matter the sequence of events – fed experiments at storage equilibrium (resets), unfed experiments at equilibrium (storms), fed experiments below equilibrium (equilibrium experiments) or unfed experiments below equilibrium (later degradation experiments) – coarse export remained between 0 – 40% of coarse import. The results from these experiments provide insight into a channel's reaction to sustained sediment starvation, which could occur as a result of an upstream dam installation (Peirce et al., 2021) or a change in hydrological flow regime.

While recovering from the degradation experiments during the second set of alternating experiments, shown in Figure 9e and 9f, the overall material export increased. The first unfed storm performed after the degradation experiments exhibited minimal fine material export, while the coarse export remained consistent with previous experiments, where the coarse fractional exports were relatively uniform. In general, the second set of storms expressed a larger degree of variability than the first set of storms. As was the case between the first and second set of storms, export fractions for the second set of resets trended upwards in chronological order, while the first set decreased with time. Another notable difference between the first and second set of reset experiments is that the peak export fraction occurred in the 0.35 – 0.71 mm range in the first set, while this range in the second set is the second lowest of the five particle classes. As in the other experiments the results from the final

experiments further suggest that the initial storage condition is important for predicting the geomorphological response of a channel.

4.2 Topographic Analysis

In this section, the results from the structure-from-motion processing are first presented as digital elevation models before being further analyzed to create sediment thickness distributions in the form of hypsometric curves.

4.2.1 Digital Elevation Models

Using the stereo camera setup, DEMs were created for each experiment. The orthomosaic images, taken once the bed had dried after each experiment, show the way the flow changed the channel's geomorphology during the experiments. Blue areas and red areas depict aggradation and degradation respectively, while darker colours signify a greater change in elevation. While the sediment export results depict sediment transport patterns from a global perspective, the topographic results provide a locational perspective. Understanding the types of locations that undergo aggradation and erosion is critical for understanding where a river's 'hotspots' of sediment transport are found. Erosional and depositional locations are intrinsically linked, as upstream patches of erosion are likely the source of material for depositional patches.

The DEMs created for the equilibrium experiments show the rapid evolution of bedforms in the first experiment, after which the development slowly tapers off as the channel's storage approaches equilibrium. Most notably, localized erosion still occurred while the bed was still filling rapidly, implying that the bed is even being rearranged during the building process.

After 180 minutes had elapsed and the first experiment had been completed, bedforms had formed in every bend of the channel, including in the most downstream bend, which was slightly underdeveloped in comparison to the upstream bends. The largest degree of deposition occurred just downstream of the bend apex, where the deepest and widest deposits were observed. Some point bars located in adjacent bends became connected by a narrow patch of sediment, while most remained disconnected. Of the two duplicate reaches, the downstream reach continued to aggrade significantly during the second equilibrium experiment, while little change was observed in the upstream bend. Overall, the bed mostly aggraded, although some smaller, isolated, and variably located areas experienced acute erosion. Laterally, more aggradation occurred along the toes of existing bedforms.

Although the feed rate and overall storage increased in experiment three, the majority of the channel's area experienced erosion, especially along the toes of bedforms. Compared to the previous two equilibrium experiments, significant aggradation occurred in smaller and higher pockets of sediment. In the final equilibrium experiment, minor rearrangements to the bed were noted despite a relatively stable storage level.

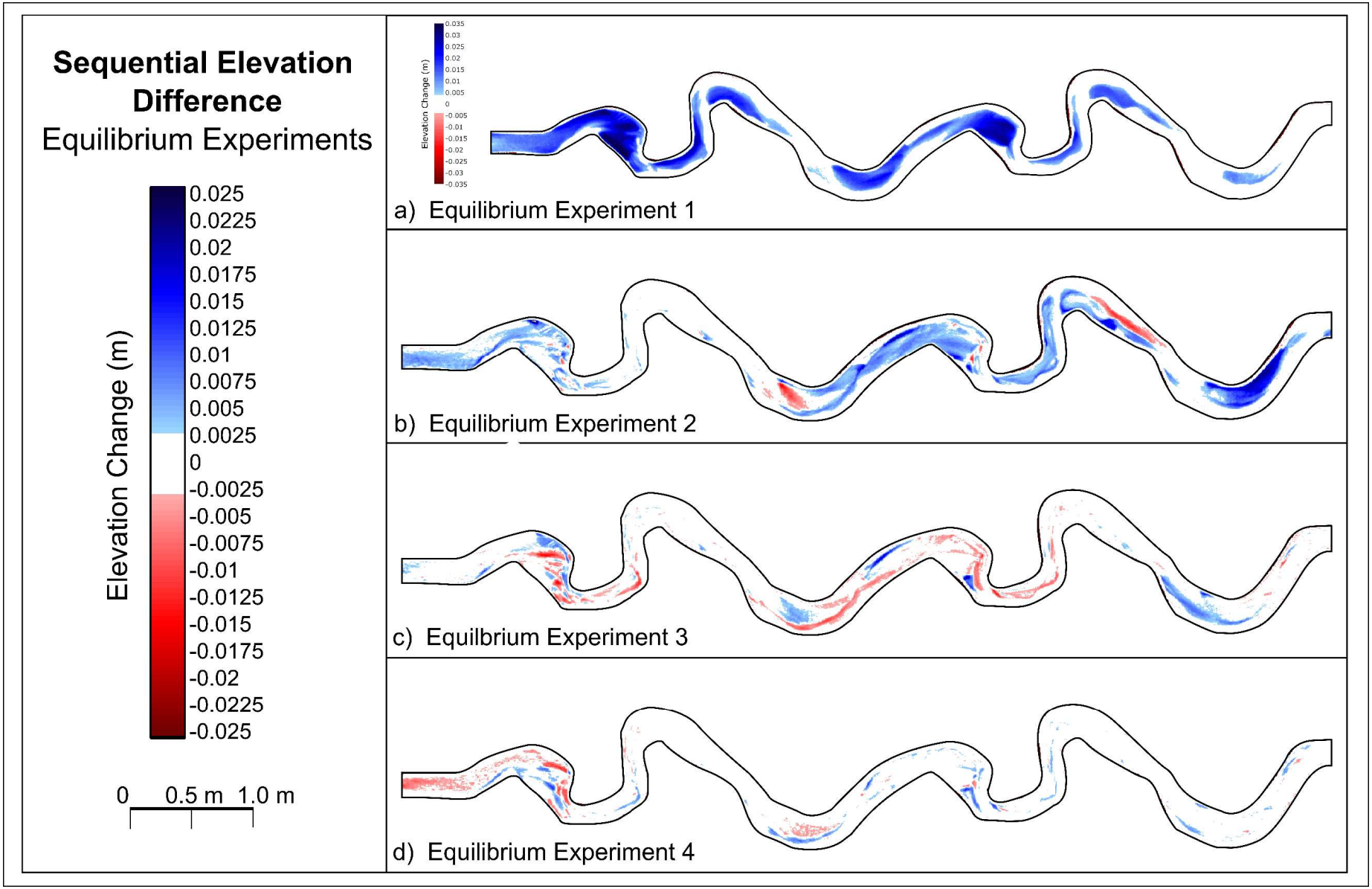

Figure 10. Sequential elevation differences: Equilibrium experiments

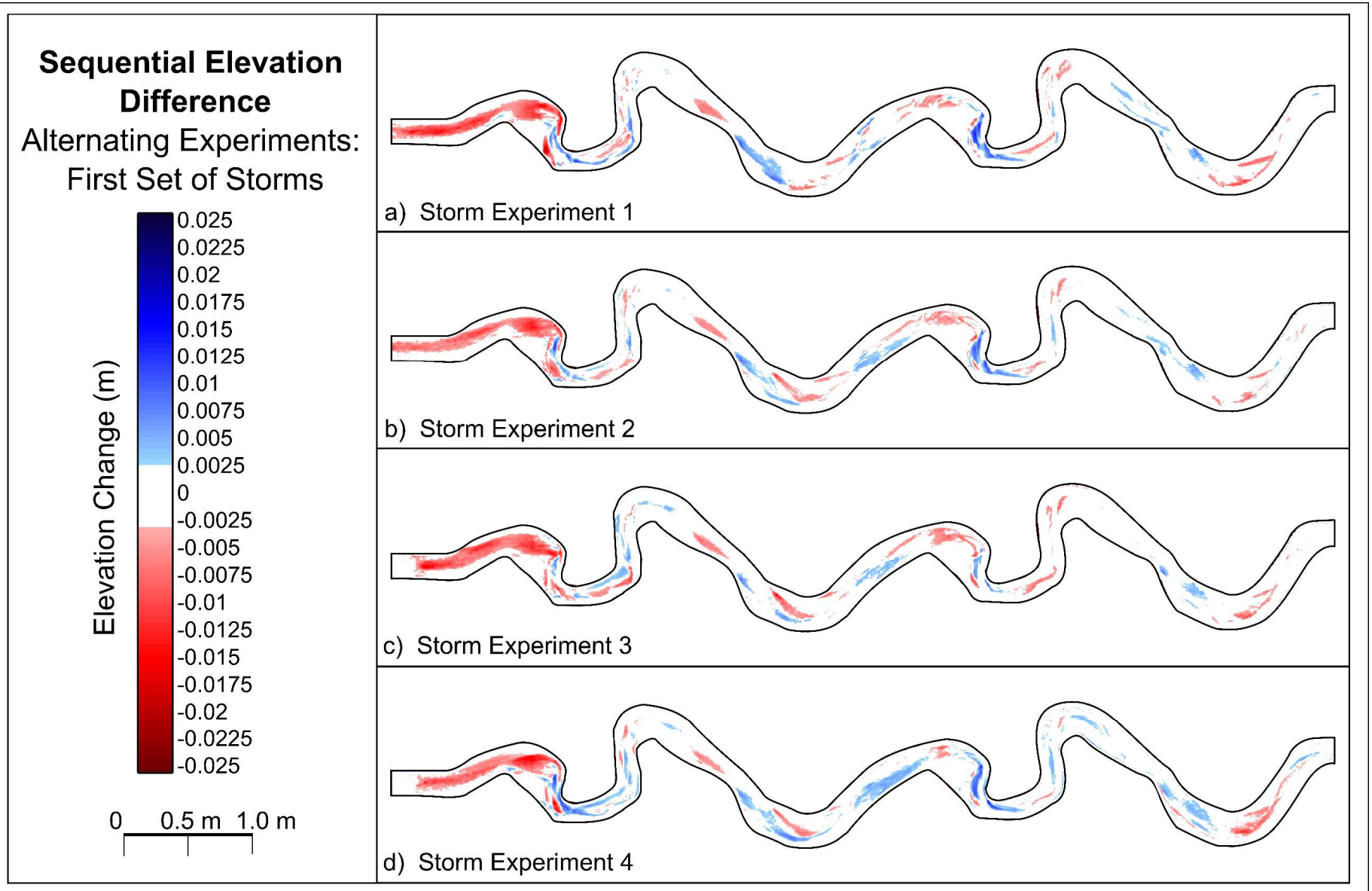

Figure 11. Sequential elevation differences: First set of storms

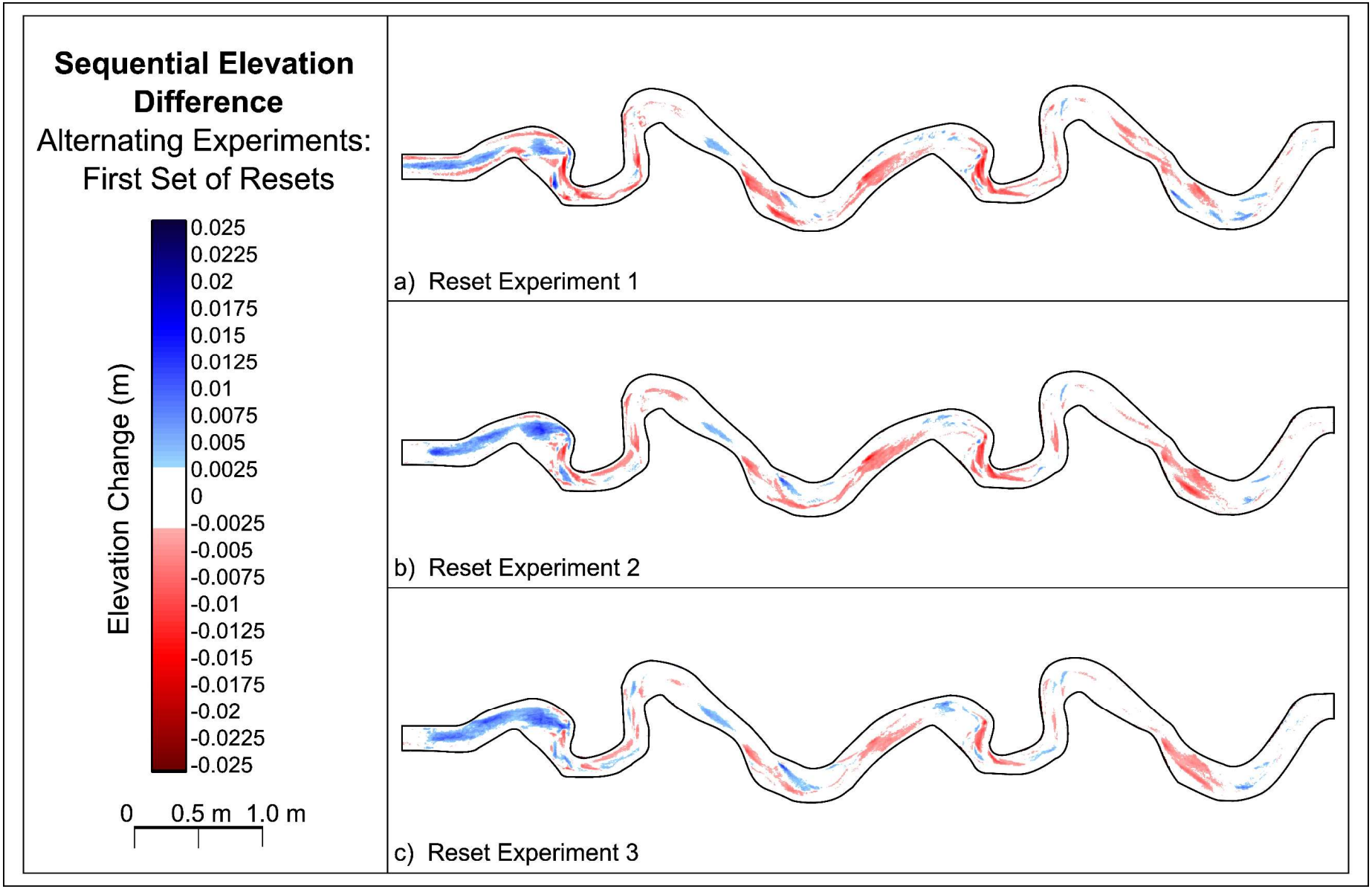

Figure 12. Sequential elevation differences: First set of resets

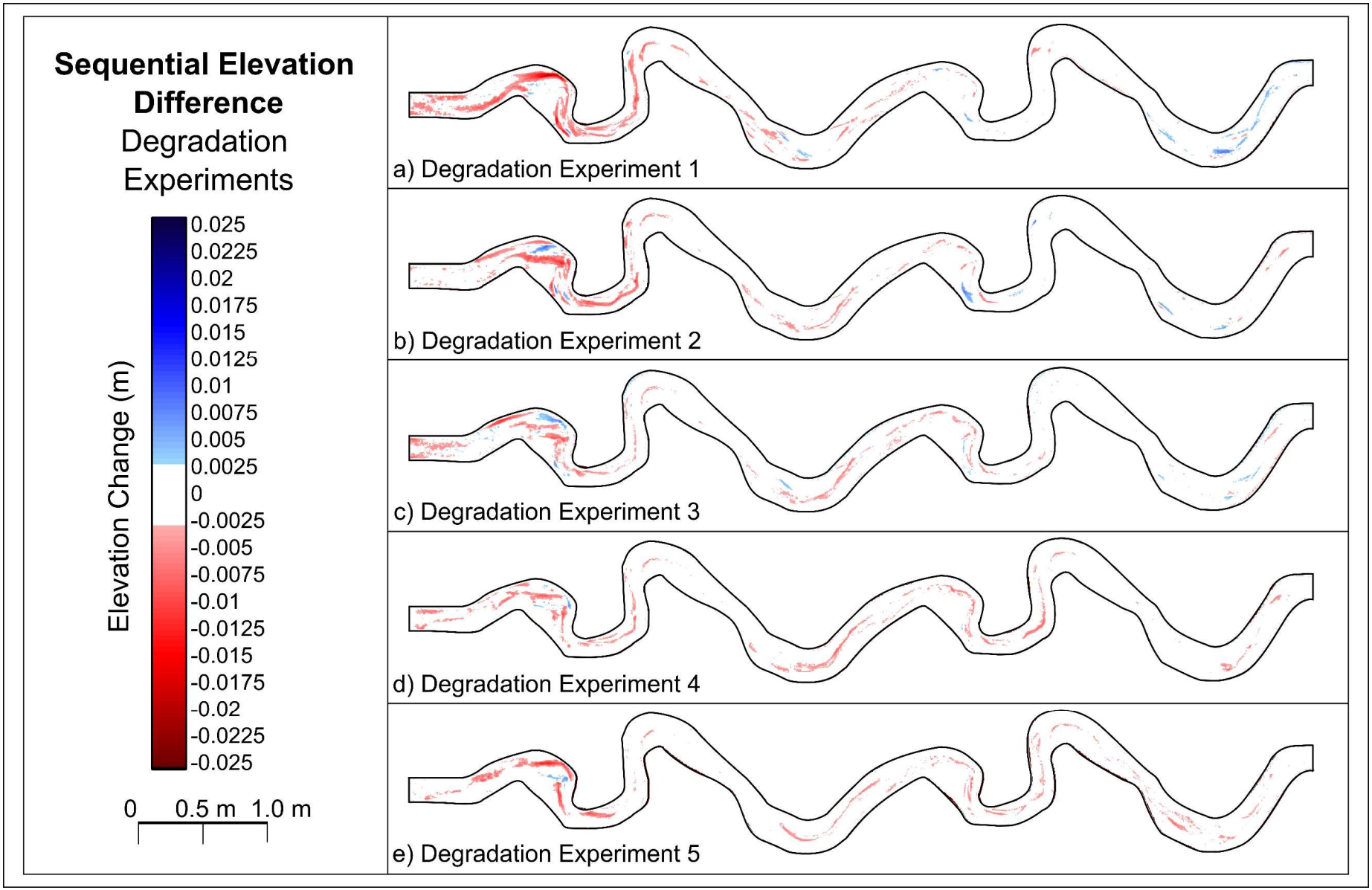

Figure 13. Sequential elevation differences: Degradation experiments

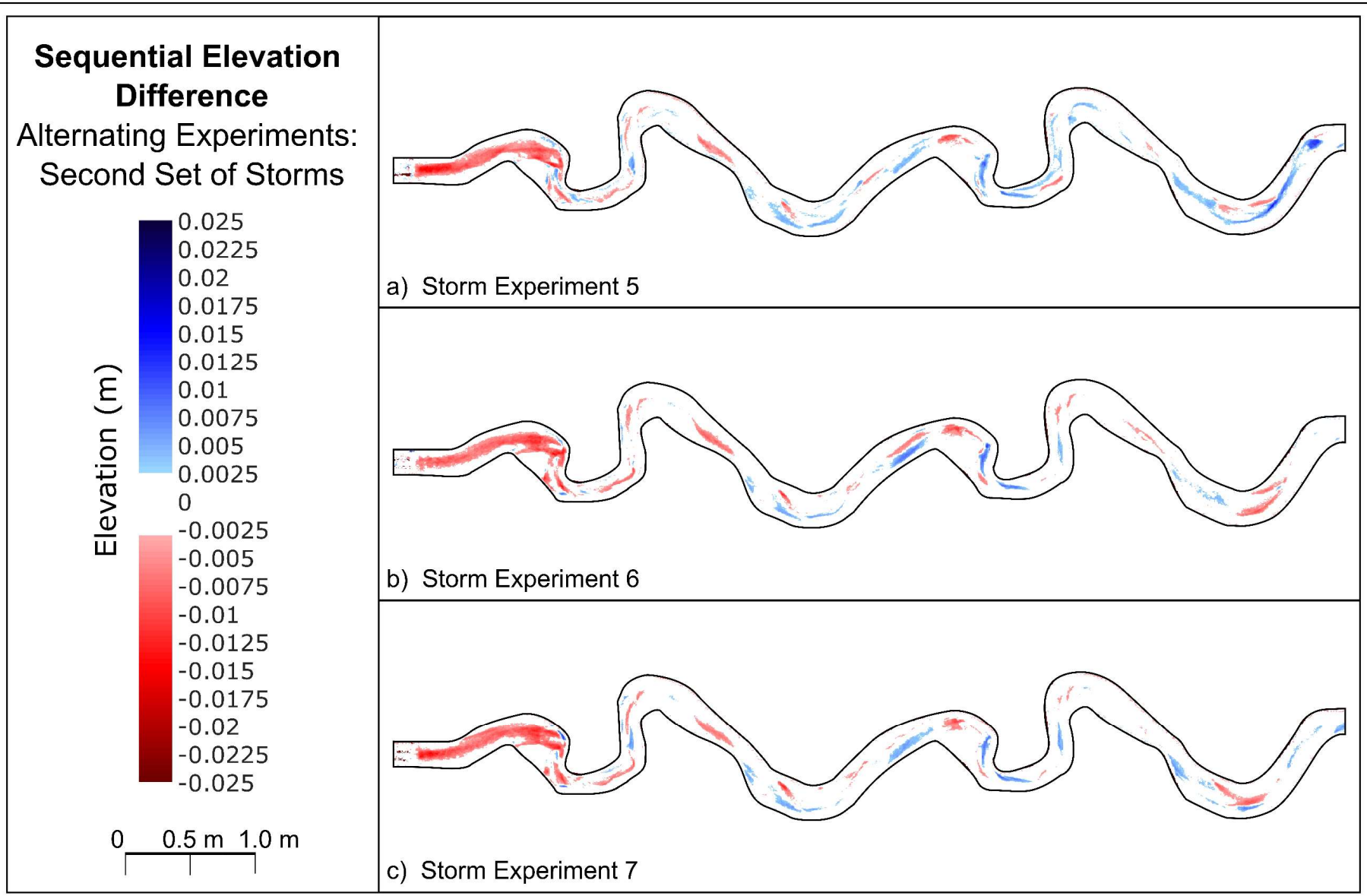

Figure 14. Sequential elevation differences: Second set of storms

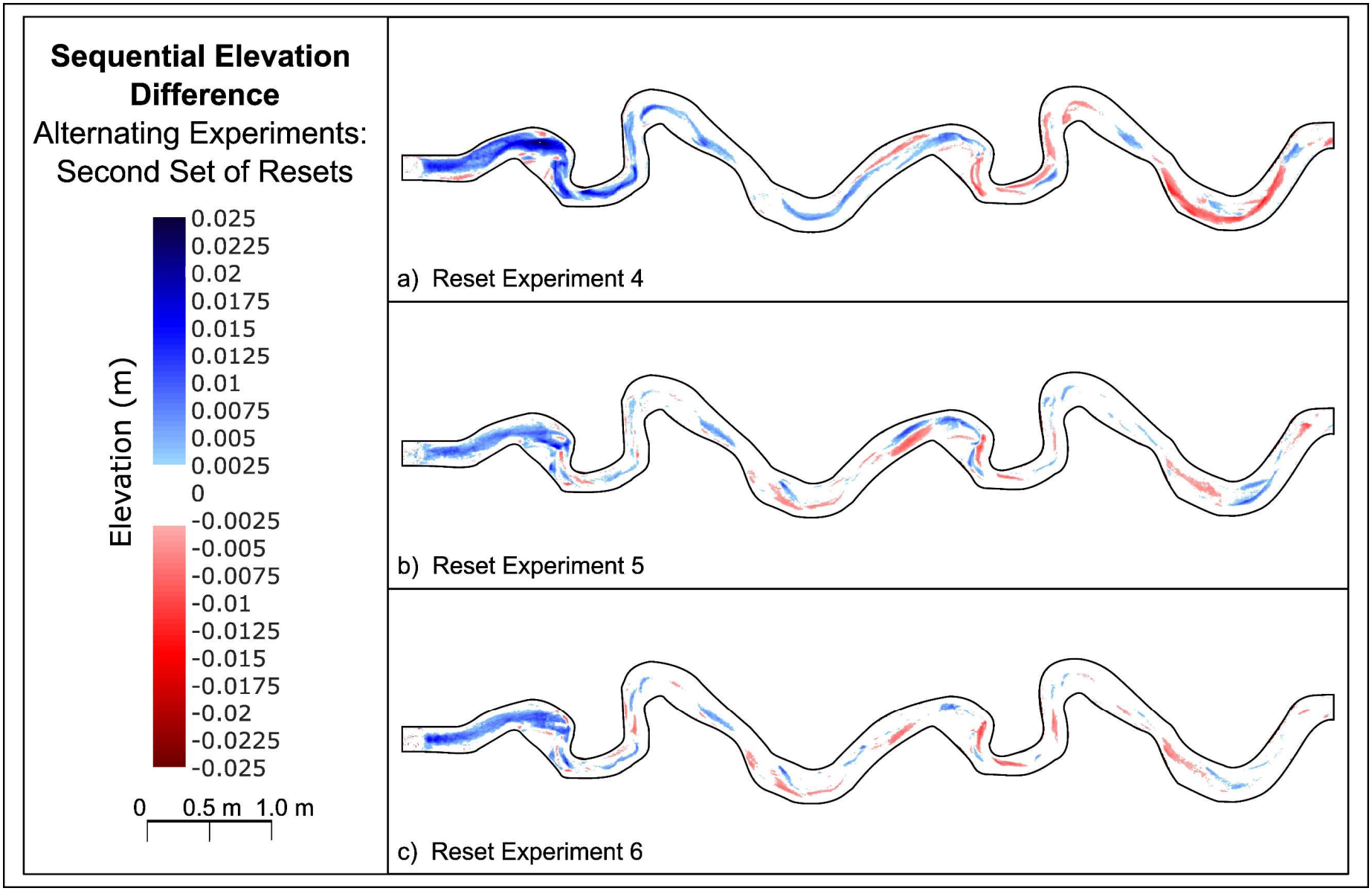

Figure 15. Sequential elevation differences: Second set of resets

Several interesting observations could be made about DEMs from the storm and reset experiments, depicted in Figures 11 and 12. Most notably, the experiments were very consistent; all storm experiments showed aggradation and erosion in the same spots. In many locations where aggradation occurred during the storm experiments, erosion would occur during the reset experiments, and vice versa. Surprisingly, the fed reset experiments showed more widespread erosion than the storm events. More erosion occurred at the toe of bars and in lower elevation areas, illustrated by a thin zone of degradation along the outside extent of point bars. Some areas connecting point bars showed slight deposition and were flanked by zones of erosion on the upstream and downstream extents. Reset experiments performed after the series of degradation experiments showed much higher levels of deposition than in those performed before and coincided with the gradual increase in total storage. Generally, it appeared that the effect of influent sediment (present during reset experiments and not present during storms) had a secondary effect when compared to the relative storage of the channel. When the storage was closer to equilibrium, both resets and storms showed high degrees of erosion. On the other hand, when the storage was lower due to the series of degradation experiments, both resets and storms displayed aggradation. Additionally, relative stage played a large part in the location of either aggradation or deposition. When the channel storage was closer to equilibrium during the first set of storm experiments, higher elevation areas displayed erosion. These areas underwent aggradation in the experiments following the degradation events.

Generally, the degradation experiments, shown in Figure 13, resulted in widespread erosion, with the exception of small areas in the downstream bends. These areas aggraded in the initial experiments due to the introduction of upstream material but began to erode more and more with each degradation experiment. Throughout all degradation experiments, erosion mostly took place along the toe of the bars. If these patterns hold true in real-world rivers, the areas undergoing high amounts of concentrated degradational forces could be enhanced with more resistant material.

A striking attribute present in each experiment's DEM is a zone of extreme activity at the upstream extent of the channel. The area, which high levels of erosion during unfed experiments and high levels of deposition during fed experiments, is located directly under and downstream of the sediment input location. Although a large fraction of the influent sediment is mobilized by the flow, a significant amount remains, likely resulting in a local exceedance of channel capacity. During unfed experiments, the deposit acts like a sediment source for downstream areas, embodied in Figures 12 and 15 in the most upstream portion of the flume.

4.2.2 Hypsometry

Hypsometric curves that describe the distribution of sediment depositional depths were determined following the method described by Peirce et al. (2021), as well as Czapiga et al. (2015), Redolfi et al. (2016), and Gardner et al. (2018). The sediment thicknesses were normalized against a representative water depth of 0.02 m. The hypsometric curves display a linear trend around the central normalized cover thicknesses, with two heavy tails at the extreme low and high cover thicknesses. While the export results provide a global perspective of sediment transport, and the topographical results provide a geographic, planform perspective, the hypsometric results display sediment transport patterns from a profile perspective.

It should be noted that the lower of the two heavy tails exists within the estimated DEM error and may not be accurate. A linear regression was fit to the central trends of the results from Peirce's three equilibrium experiments. These linear relationships were plotted on this study's hypsometry figures, displayed on the following page in Figure 16, to aid in comparison between the two studies. To aid in the discussion, we will refer to low, central, and high cover thickness zones as those below 0.5, between 0.5 and 0.75 and above 0.75, respectively. Thickness variability within the DEM error will not be discussed.

The rapid evolution of bedforms occurring during the initial equilibrium experiment is apparent in the hypsometry relationships, which increase in conjunction with the previous storage relationships. Over 40% of the bed was covered with a minimum thickness of 5 mm after the first experiment. Future experiments performed in this study do not exceed a cover percentage of 60% at this cover thickness, making it evident that the majority of bedforms developed in the first experiment. After reaching equilibrium at 4 g/s, after the second equilibrium experiment, the hypsometric curve is very close to Peirce's 4 g/s line, with some minor differences.

A characteristic response to storm events is apparent in the hypsometric results of the alternating experiments. As the storage in the channel decreases with each new set of alternating experiments, the relative cover thickness decreases. Compared to the state of the bed before the first storm, the hypsometric curve after the storm is steeper, with higher bed coverage in the low thickness range below 0.5, while thicknesses in the central and higher regions (above 0.5) degrade slightly. The subsequent reset experiment displays the opposite result: a loss of thickness in the lower range and an increase in the central mm range. The first reset experiment also displays degradation in the higher

thickness range. This trend continues through the first set, with each storm developing topographically lower areas, before the following reset degrades these areas and fills in the lower and central ranges. After the fourth storm, the degradation experiments were performed, which are discussed in the following section.

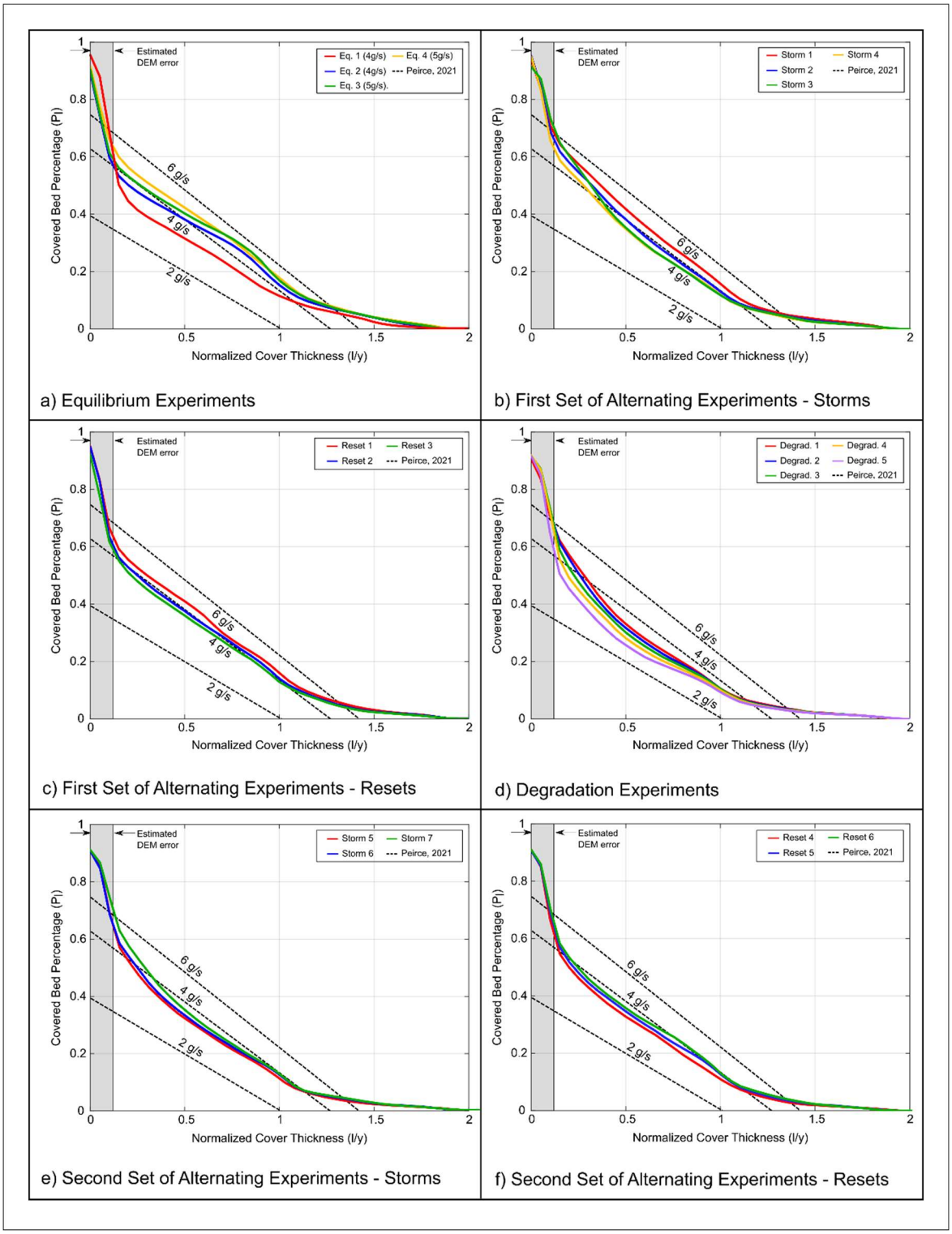

Figure 16. Hypsometry for each experiment type, depicting the statistical distribution of sediment thicknesses in the channel.

After each degradation experiment, the overall cover thickness was less than before beginning, although some thicknesses degraded faster than others. Most notably, the lower and central zones degraded the most, with the degradation in the higher regions plateauing as more experiments were performed. The high thickness areas above 0.75 experienced cover degradation between 1 – 5%, while the lower and central cover decreased by 10%. Due to this preferential decrease in thickness, the linear trend of the hypsometric curves became less apparent with each experiment, resulting in a steepening trend in the lower regions and a flattening trend in the higher regions. The degradation effect also became faster, as the curves became increasingly farther apart in the lower regions.

During the following second set of alternating experiments, each storm-reset pair displayed a net growth, as the channel storage began below the equilibrium storage level and tended towards steady-state over time. In contrast with the first set of alternating experiments, the low thickness zones were relatively insensitive to change, while the central thickness areas evolved in a similar manner: thicker after the resets, and thinner after the storms. The degradation effect is most noticeable in the low elevation areas along the face of bars. The channel is incising and leaving terraces, and the erosion is not completely replaced by subsequent resets. Oftentimes, river scientists attempt to evaluate a channel's stability conditions by determining whether certain phenomena are occurring (terracing, entrenchment, or migration as a result of increased or decreased sediment concentrations), commonly referred to as a Rapid Geomorphic Assessment (RGA) (State of Maine DEP, 2007). This study allows for the analysis to be performed from the other direction, having the prior knowledge of whether the channel is in a state of starvation or whether the channel is nearing equilibrium storage.

4.3 Particle Tracking

The pathways of orange and green particles, representing the 1.18 – 2.36 mm and 2.36 – 4 mm size classes were tracked at fifteen different times during the storm experiment. The pink particles, representing the 4 – 5.6 mm size class, were found to rarely move, and therefore did not provide much insight into general sediment routing trends. Each set of particle tracks, coloured by each particle's speed, was plotted overtop the bedforms present in the bend during each ten second clip. The results show routing trends quite well, with several particle pathways extending long distances at a variety of speeds, although there are some limitations. Due to surficial turbulence and, in some cases, a high degree of particle activity, particle tracks often became disconnected during plotting, exaggerating the amount of particle pathways and underrepresenting the length of each path. This

error was found to increase as the number of particles in the active frame became larger. This became more apparent at the colour thresholding stage, where particles in crowded areas began to flicker. In addition to overcrowding, some isolated particles located in more inactive zones were observed to 'vibrate' and were portrayed as small dots with low velocity. Due to the lack of understanding surrounding the source of the vibrating particles, they were included in the sediment tracking figures. Particle tracking figures for the orange and green particles filmed at ROI 1 are presented on the following four pages as Figures 17 through 20. Understanding where particles are being transported allows for the delineation of a transport zone, not only shedding light onto existing theories of sediment transport, but also theories involving flow convergence and divergence.

In consideration of these limitations, several interesting observations were made regarding the routing of sediment through the channel bend. As expected, the overall particle activity increased with discharge. The initial surge of water, which cleared out a small amount of sediment collected in the bend during the drawdown of the previous experiment, caused some particle movement during the first clip (a). After this initial surge, no movement was observed until approximately halfway up the rising limb of the hydrograph. At this point, patterns in speed with respect to the particle's location on the bed became apparent. In both the orange and green results, particles approached the downstream end of the point bar with relatively high speeds, before slowing down over the bare section between the two point bars. After crossing the bare section, the velocity of the sediment increased again as it moved along the point bar. This slowing phenomenon continued as the space between the upstream and downstream point bars filled in. Several fast tracks were located at the crossing during the peak, but due to the direction and the length of these paths, it is thought that they are a product of error due to significant turbulence and particle activity. Although patterns between speed and location were obvious, no discernable difference in particle speed was found at different discharge levels. Although the number of particles travelling increased and decreased with discharge, particles travelling at lower discharges still reached the same speed as observed at higher discharges.

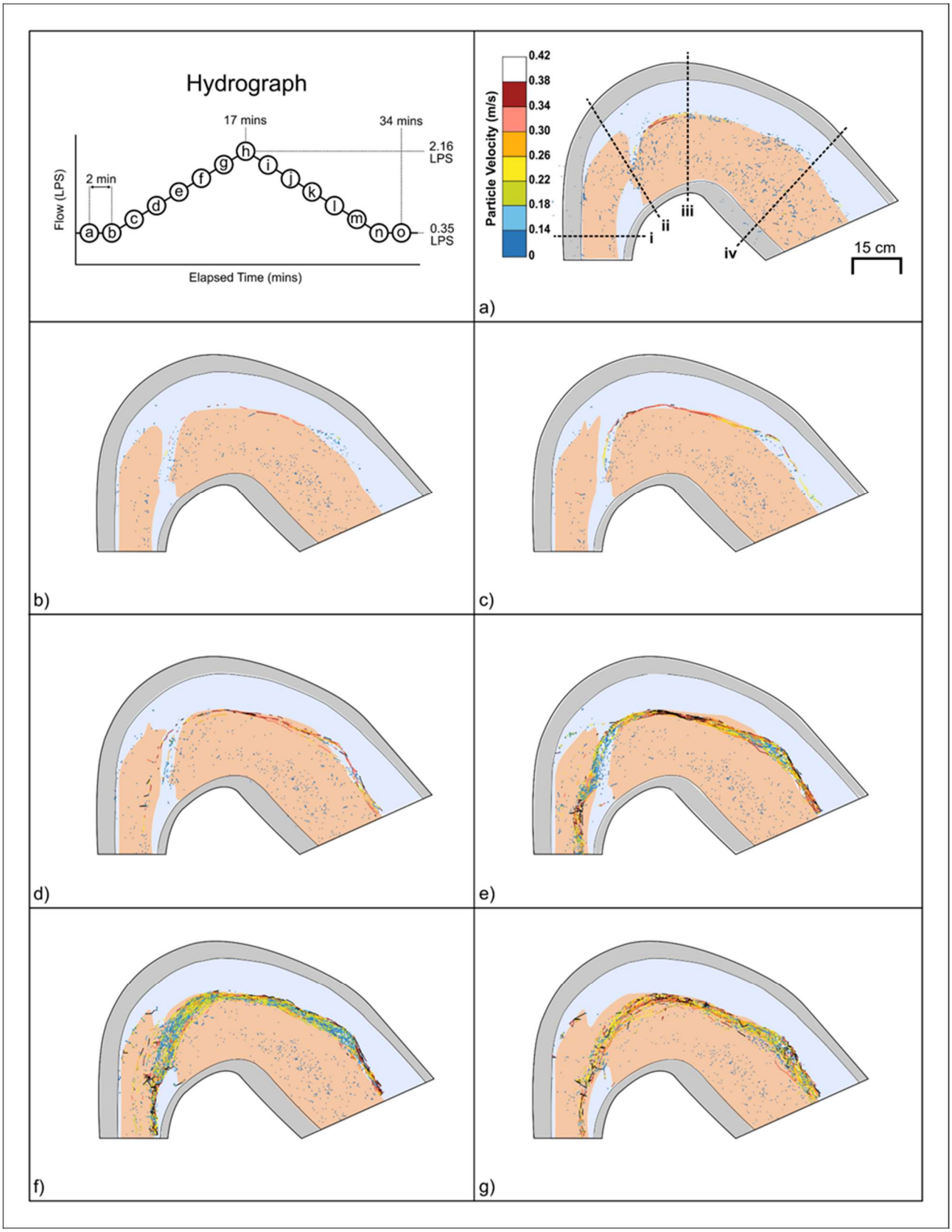

Figure 17. Particle tracking of orange particles at ROI 1 during storm - Part 1

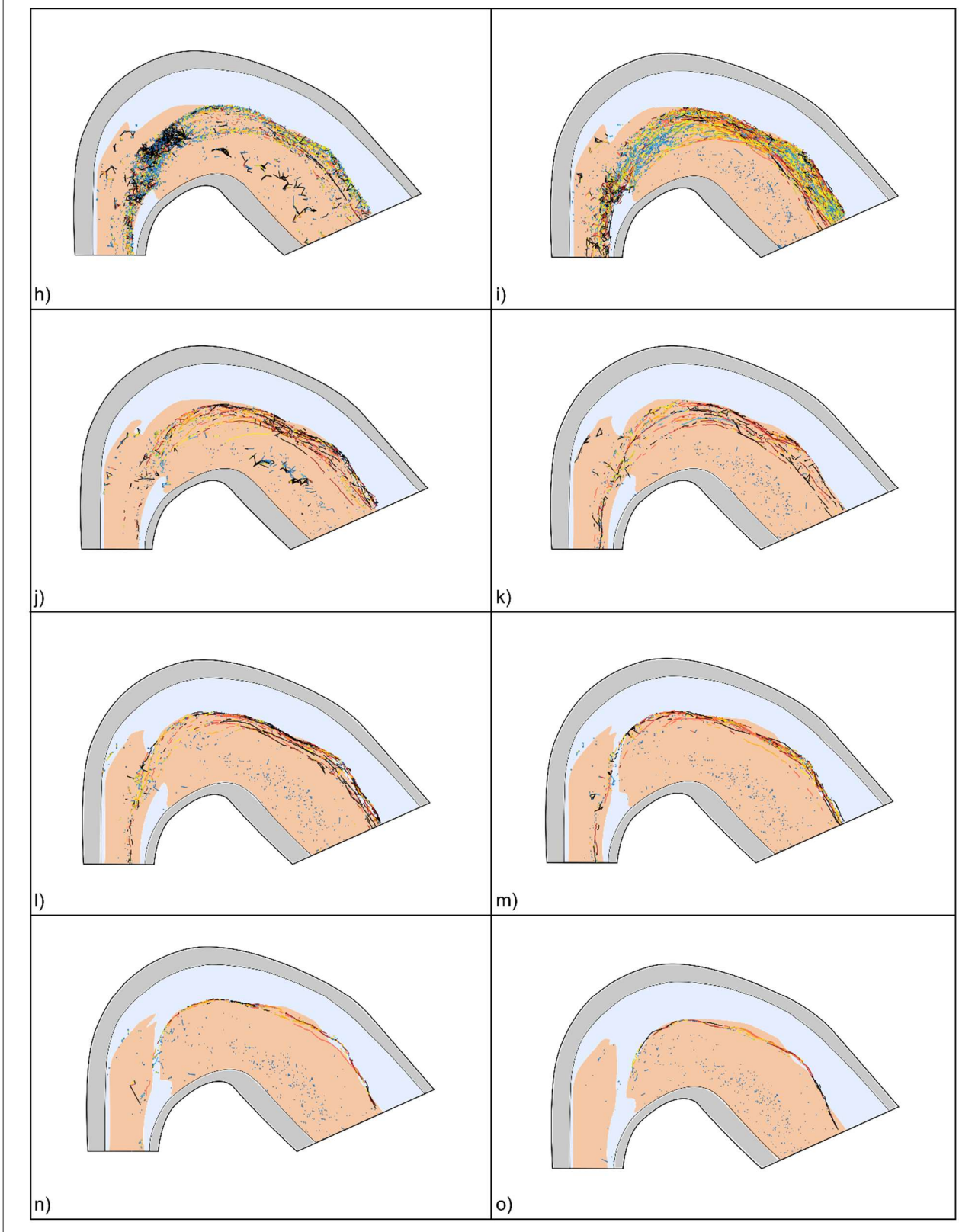

Figure 18. Particle tracking of orange particles at ROI 1 during storm - Part 2

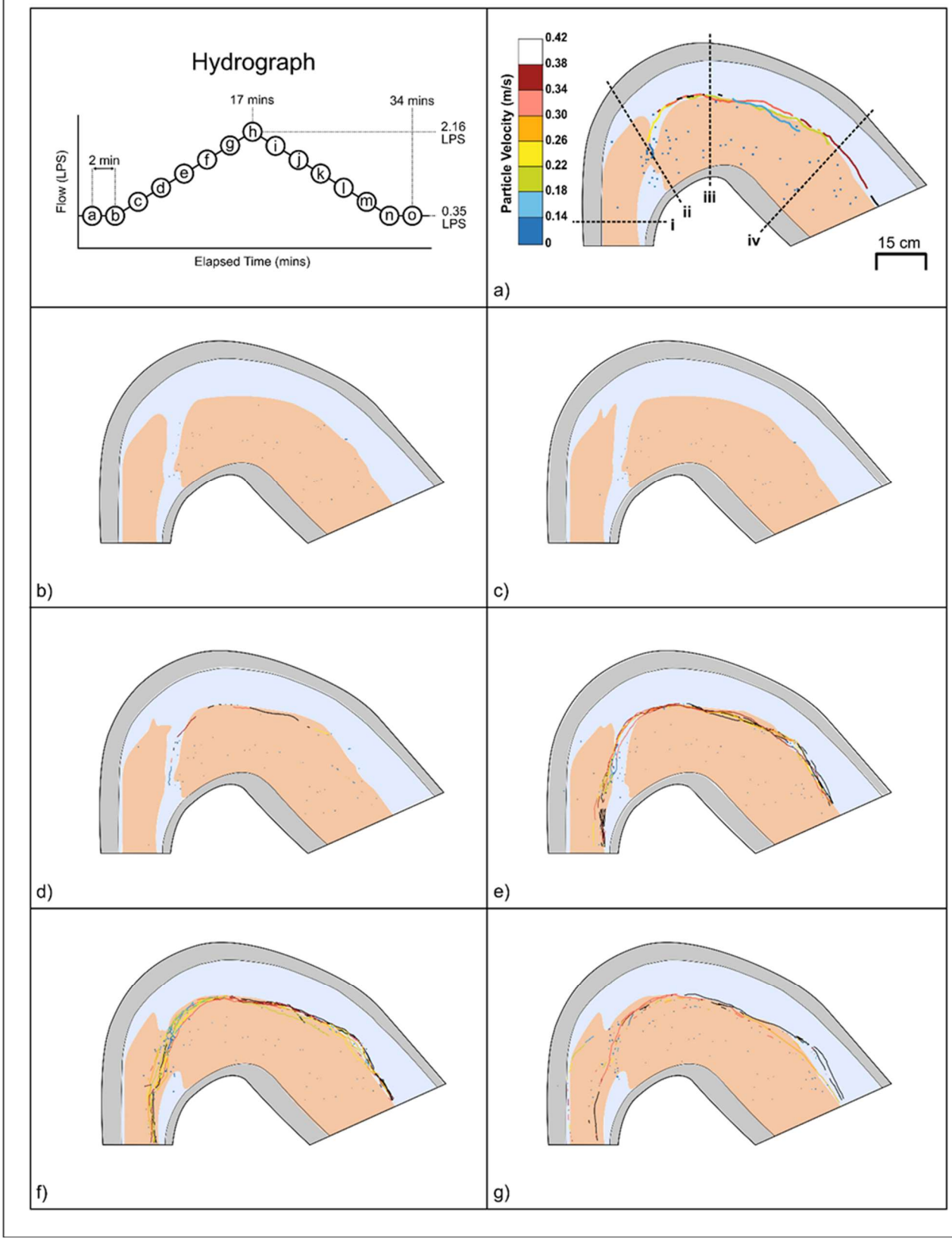

Figure 19. Particle tracking of green particles at ROI 1 during storm - Part 1

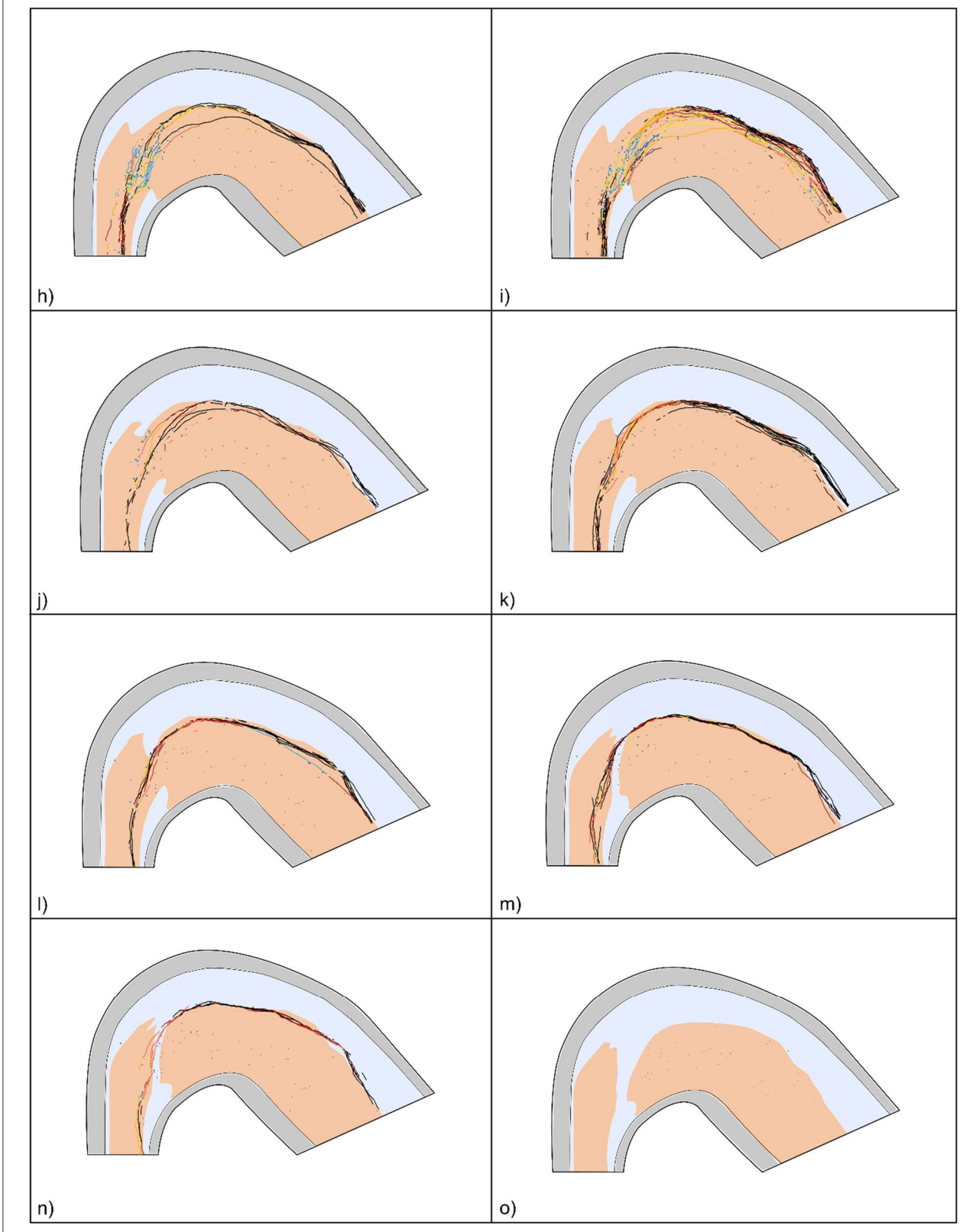

Figure 20. Particle tracking of green particles at ROI 1 during storm - Part 2

Another characteristic of the travelling particles that produced notable results, and had a strong correlation to discharge, was the active transport zone. As seen in all tracking figures, no particles were observed to travel into the bend's outer zone. Although almost half of the channel was uncovered during the experiments, particles did not deviate from the toe of the point bars, and exclusively travelled over area covered by sediment. Where this was not possible, namely at the crossing between point bars, particles seemed to take the shortest path between covered zones, and quickly covered the area between the bars as activity increased. At all times, the active lateral width of transport was limited by the toe and the stage of the water. As discharge and stage increased, the active transport zone became wider, moving laterally towards the inside bank of the bend. The widest active transport zones occurred over the connection between point bars, where particles appeared to slow down and spread out laterally. After crossing the connection, particles narrowed again as they travelled downstream. This pattern was most apparent during the clips surrounding the peak (g, h, and i). As the stage decreased, the patterns mirrored those observed on the rising limb as the connective patch dissolved, and the area between the point bars became bare once again. This event coincided with the gradual decrease in particle activity over the area between point bars.

In addition to the sediment's speed and active zone, the general orientation of the pathways also changed with discharge. At lower discharges and stages on the extremities of the rising and falling limbs, particles tended to travel along the upstream bar for longer, only crossing once the terminus of the bar was encountered. This resulted in a pathway that was oriented almost perpendicular to the valley trend. As the discharge increased, and the active zone of transport widened, the zone of transport tended in the direction of the valley trend as particles began to cross over to the downstream bar before the terminus of the upstream bar was reached. Interestingly, the general direction of sediment transport shifted towards the inner bend such that the zone was no longer limited by the toe of the bar, leaving an area on the bar untraversed by sediment. This mainly occurred just downstream of the connection between the point bars. As discharge and stage began to decrease, the general path of particles returned to the previous, perpendicular orientation.

Chapter 5 Discussion

The overall goal of this study was to understand the formation of riffle-pools so that a restoration strategy based on sediment feeding could be proposed. The viability of such a method relies on understanding the mechanisms behind erosion and deposition in rivers, and where they take place in partially alluvial channels. After presenting evidence for the reproducibility of flume experiments, the viability of previous theories behind these mechanisms are discussed. Finally, these discussion points are put into context of restoration efforts in rivers.

5.1 Reproduction of Flume Experiments

The first objective of this study was to reproduce the results obtained by Peirce et al. (2021), thus assessing the reproducibility of flume experiments. Several obstacles must be overcome to achieve this, including but not limited to the differences in flow rate, experiment length, sediment type, and sediment feed rate. Once these parameters have been considered, it remains that the experiments must be observed in a similar fashion, ideally with similar video recording apparatuses, bed photography, and sediment sampling intervals. In an attempt to replicate a previous flume experiment, these parameters were identified in Peirce et al.'s experiments (2021) and applied to the equilibrium experiments. Consequently, the results from these experiments were analyzed and presented in a similar fashion. Figures published by Peirce et al., depicting the sediment storage over time, the relative export of individual grain size classes, and the relative depth of sediment throughout the channel, were replicated for the equilibrium experiments. These quantitative methods of analysis are also supported by patterns that were visually identified in both studies. Peirce et al. cited the presence of 'diagonal, riffle-like structures' that formed between point bars in series to one another. These cross-over structures were described to be analogous to riffles fitting the description of classic pool-riffle morphology as per Thompson (2018).

5.1.1 Overall Sediment Storage

Although sediment storage was tracked from the initial, empty bed state in both experiments, as seen in Figure 8, the Peirce et al. experiments (2021) were stopped after reaching a state of sediment transport equilibrium, while the experiments performed in this study preceded several other experiment types. After the experiments were initiated, both storage relationships depict a steep incline, matching each other very closely. Since no sediment export had been observed during this linear period, the extreme similarity between the two curves (below 1% difference) indicates that the

influent feed rates are very similar. Although sediment begins to exit the flume 30 minutes earlier and at a storage level of 3 kg lower in this study than in Peirce et al., the relative difference between the two studies remains below 5%. Nonetheless, the difference between the overall storage levels at the end of both 4 g/s experiments suggests that, in this study, equilibrium was not reached in the same extent as it was in Peirce et al.'s study. A key difference between the two studies is the frequency of bed photograph, and thus the frequency of pump cessation and drawdown. In the studies performed by Peirce et al. (2021) the pump was turned off every 20 minutes for the first 3 hours, and every 90 minutes for the remainder of the experiments. The drawdown may have affected the results such that the storage capacity for each study was different. Other small differences between the two studies include the potential of small differences in flow rate, which would alter the carrying capacity of the channel (Einstein, 1950), or even localized bifurcations, which could increase or decrease the storage capabilities of large bar formations.

Although most of the results were similar between replicate experiments, some differences were noted. In the third storm experiment, large particles deposited between bars, and were quickly filled in with fine material. As flow increased, the patch increased to a point where the upstream and downstream bars were observed to grow laterally. In the fourth storm experiment, large particles were also deposited, but were consequently remobilized as the flow increased. The patch formed later in the experiment but was much smaller than in the third experiment. Due to these bifurcative behaviours, it can be inferred that other regions in the flume are also sensitive to initial conditions, where the growth or degradation of a bedform could depend on a small amount of 'keystone' particles.

5.1.2 Export Fractions by Grain Size

Additional results concerning sediment import and export were produced by splitting the exported material into size classes. While Peirce et al. (2021) provided data from the last five sampling points – during which the bed state asymptotically approached equilibrium – all sampling points were provided in this study's analysis to further investigate the effect of bed state relative to equilibrium state. Results between the two studies are very similar: medium sized particles were observed to reach equilibrium, as export fractions for particles between 0.35 mm and 2.8 mm were equal to 1 ± 0.05, while both coarse and fine particles were significantly below 1. Peirce et al.'s results are most appropriately compared to this study's 4 g/s equilibrium experiment – experiment 2.

Although the general trends between the two studies match well, less export was observed in both the coarse and fine fractions during this study's experiment. This lack of coarse and fine export is interesting, as the overall storage relationship depicted more export in this study than in that performed by Peirce et al. Two main reasons can be provided for this contradiction. The shape of the overall storage curve suggests that export began earlier, resulting in an overall lower storage at the 4 g/s equilibrium bed state. The discrepancy between the two studies' export fractions suggests a lower export rate and does not consider the time at which sediment export began. Additionally, the standard error presented by Peirce et al. extends the range of fine material export fractions to just above 0.4, which is much closer to the fine export fraction in this study. Discrepancies aside, this study supports conclusions determined by Peirce et al., such that coarse and fine material classes play large, yet different roles in bedform formation, shown by their decreased rate of export. Evidence provided by video recordings and the export fraction analysis support that coarse material is responsible for creating a framework, while fine material fills in the gaps, increasing the extent and height of bedforms. The 5 g/s equilibrium experiments performed in this study expand on these mechanisms, as a higher feed rate brings the channel closer to its sediment carrying capacity, resulting in a greater export of unneeded formative (fine) material. Fine material export in the 5 g/s experiments increases as time passes, exceeding the export fractions reported in Peirce et al.'s 4 g/s experiments. The export of coarse material in the 5 g/s experiments remains unchanged, which supports Peirce et al.'s conclusion that the transport is coarse material is simply much slower, and that the continuous accumulation of coarse material indicates a potential for further morphologic dynamics.

5.1.3 Hypsometry

The hypsometric analysis performed in Peirce et al. (2021) provides insight into the distribution of sediment depth throughout the channel. Interesting connections can also be drawn between the elevation of degradation and the size distribution of exported sediment. Degradation that takes place closer to steady-state and is accompanied by aggradation on downstream bars results in export with an even size distribution. Erosion occurring after the sediment storage has dropped significantly below an equilibrium state results in a more uniform degradation of all bars, while the export of fines drastically increases and the coarse export drops slightly. Therefore, it can be inferred that the upstream end of the flume undergoes rapid erosion, and the resulting pulse of fine material acts as a sediment source to downstream bars. The hypsometric results indicate that the majority of upstream degradation and downstream aggradation occurs in lower elevations. The erosive front continues to

travel downstream over time until the end of the flume is reached, and the fine material is reflected in the export fraction results.

Results from the equilibrium experiments, shown in Figure 16, provide the comparison of channel hypsometry present in the two studies. The two hypsometric relationships for the two studies' equilibrium state 4 g/s experiments are similar, although this study's curve depicts a greater frequency of thicker bedforms and a lesser frequency of thinner bedforms. In the hypsometric figure, this difference results in a flatter slope than observed in Peirce et al.'s experiments and can be linked to the lesser export discussed previously. If sediment is stored at higher elevations, it becomes less exposed to depth-proportional shear stresses. Contrarily, the deficit appears to be compensated for in the lower regions, which display more erosion than reported in Peirce et al.

The 5 g/s hypsometric curve approximately settles between the 4 g/s and 6 g/s experiments completed by Peirce et al., (2021). The steepening of the hypsometric curve, seen during the increase in feed rate, also aligns with Peirce et al.'s theory that sediment starvation leads to a flattening in tangential hypsometric slope, first discussed in reference to a river with a large dam. The result in this study further confirms that a sudden decrease in sediment supply will cause degradation of lower bedforms, while leaving higher elevation bedforms untouched. This effect could result in steeper bank and bar angles, potentially causing greater channel instability.

5.1.4 Topographic Analysis

Since several repeat experiments were run, the DEMs can be compared to one another to determine the repeatability of experiments. Generally, the DEMs of the reset and storm experiments are consistent in their type, with small discrepancies likely arising from the relative storage of the channel. Small erosive or depositional patches are present in the same location throughout most similar experiment types, except for during the equilibrium and degradation experiments, where the channel storage changed significantly throughout the experiments.

The topography after degradation experiments confirms the results from the hypsometry, as an erosive front is observed to move downstream over the span of the experiments. This phenomenon is displayed in Figure 21 below. In the first degradation experiment, aggradation due to upstream erosion is observed, while in the last experiment solely degradation can be seen. This discrepancy occurs gradually over the five degradation experiments. The aggradation and erosion occurring around the front takes place at the fringe of the bars, where the sediment thickness is the smallest.

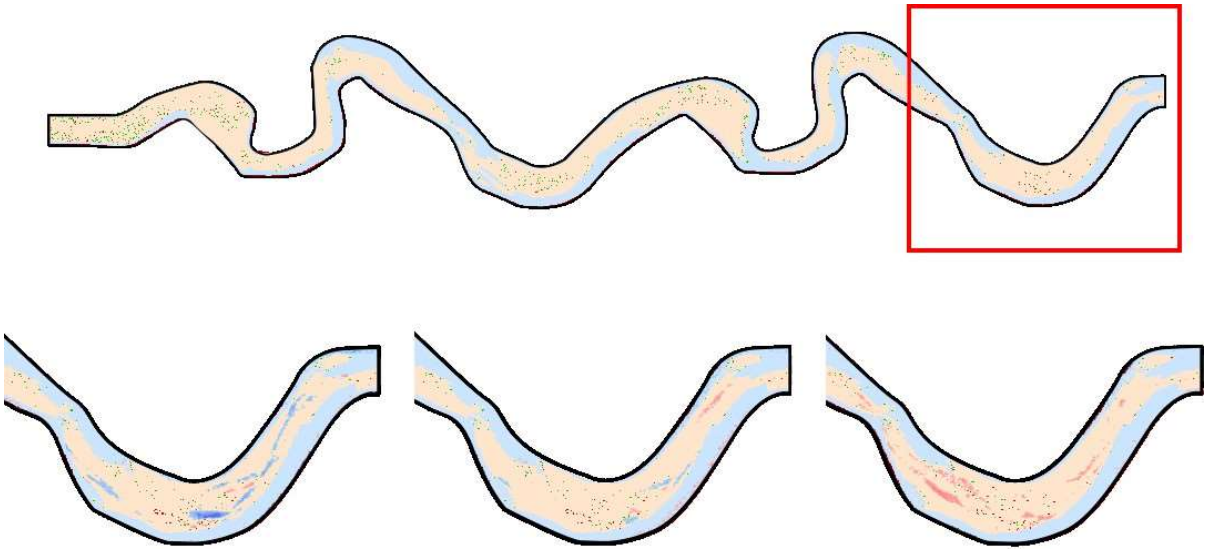

Figure 21. Erosion (red) and deposition (blue) at downstream end during the first (bottom left), third (bottom middle), and fifth (bottom right) degradation experiments.

An issue that arises out of most flume experiments, and one that calls into question the DEMs produced in this study, is the drawdown effect. A unique problem to flume experiments, the drawdown effect occurs when water is shut off and the draining of the flume alters the bedforms in the channel, introducing new mechanisms that were not present during the preceding experiment. This issue is not easily eliminated, as the stereoscopic method of producing the DEMs – as well as several other methods of observing channel topography – does not penetrate the water surface, and cannot be calculated while the water is running. Clearly this is a well-defined gap that exists in the methodology of flume experiments, and may require the introduction of novel techniques, such as the use of a correction factor to account for water refraction as described in Helm et al. (2020).

5.2 Pool-Riffle Maintenance Hypotheses

One of the main objectives of this study is to weigh two proposed theories behind pool-riffle maintenance: the velocity reversal theory as described by Keller (1971), and the sediment routing theory as described by Milan (2013). In addition, studies discussing the way in which sediment travels through beds is also of interest, such as Turowski (2018) and MacWilliams (2006). Many facets of these theories appear to be mutually exclusive in relation to each other. The velocity reversal

theory involves particles travelling towards the outside bend and into pools as discharge increases, and Turowski's theory concerning bedload-impact-driven erosion relies on the idea that particles deflect towards the outer bank due to inertial forces. Contrarily, Milan's sediment routing theory describes how the sediment transport path shortens with an increase in discharge, and how the direction tends towards the valley trend as the increased stage provides sediment access to topographically higher areas.

The results from this study are clearly in support of Milan's sediment routing theory. Every particle tracked during this study was routed along or over bedforms along the inner bank. Sediment deposits occurred between point bars, forming riffle-like structures, without the particles being flushed out of the upstream pool as theorized by Keller's study on velocity reversals (1971). As discharge increased, particles did not deflect from the thalweg towards the outer bank as described by Turowski (2018). Instead, the opposite occurred, as sediment transport expanded laterally towards the inner bar as stage increased, while remaining limited by the extent of the bar. Additionally, the general direction of transport deflected further away from the outer bank, tending towards the general valley trend. This mechanism is clearly shown in Milan's schematic describing sediment routing theory, where sediment begins to take the shorter path overtop of bars.

The difference in cover between the experiments performed in this study and those in Keller's (1971) and Turowski's (2018) may in part explain the discrepancies regarding sediment transport. During all experiments performed, a large region of the bed did not become covered with sediment. Since most particles travelled along the toe of point bars, it would be valuable to observe what would happen if the sediment feed rate were increased to a point of complete coverage in the channel. At this point, it is possible that particles would impact the outer wall, as per Turowski. It is also likely that velocity, shear stress, and sediment transport reversals would play a larger role in maintaining pools and riffles, as per Keller. Additional research concerning the absolute carrying capacity of the experimental channel, given large flows, would allow for these types of experiments to be carried out.

Tracking data also supports the hypotheses by MacWilliams et al. (2006), who used results from two- and three-dimensional models to establish that flow lines diverge between the pool tail and riffle head and converge between the riffle tail and pool head. To confirm the visual impression of divergence and convergence, the widths of active sediment transport zones were measured across four different cross sections: the upstream bar and pool tail (section i), across the riffle (section ii), and two sections

in the downstream bar and pool (sections iii and iv). Widths were measured for each tracking figure, providing active transport widths for several stages and discharges. Widths were normalized against the average bottom width of the channel, determined to be 230 mm by Peirce et al. (2021), while discharges were normalized against 2.16 LPS, or the peak of the hydrograph. Normalized sediment transport widths were then plotted against normalized discharge and fitted with linear correlations. Coefficients of determination (R^2 values) were calculated for each correlation and ranged from 0.52 to 0.77. As seen in Figure 22, a positive relationship exists between discharge and transport zone width throughout all cross sections. Although it is unclear whether the correlation between the two parameters is linear, a line of best fit was used to display the positive relationship. More significantly, the transport zones over the riffle were greater than all other locations throughout the entirety of experimentation. Additionally, the active transport width increased faster over the riffle than at the other cross sections, taking up 10% more of the average channel width than the second widest section at higher flows.

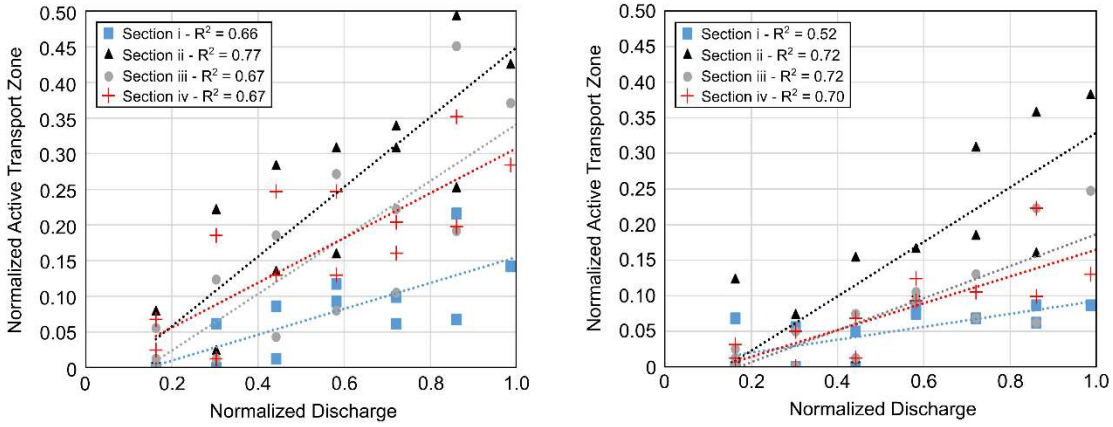

Figure 22. Normalized active transport width vs. normalized discharge (orange left, green right)

The tracking images also show significant amounts of shorter, lateral movement of particles over the riffle, suggesting that particle interactions due to increased local activity spread out the active zone of transport, in addition to flow convergence and divergence. These results have implications for one- and two-dimensional modelling of shear stresses and sediment transport. If a lateral component is not integrated into models, they will fail to capture the variability of sediment transport across the channel width. Using one representative shear stress value for the entire width of the channel will

greatly overestimate the sediment transport in most areas across the channel width, while underestimating transport in the narrow active zone.

5.3 Implications for Restoration

Although the use of a scaled down physical model will never perfectly characterize a real-world channel, several results can be gleaned from the experiments performed, and applied to the restoration efforts.

If general bedform remediation is the goal, the import – export graphs may be of interest. Most of the channel's geomorphologic structure was formed within the first equilibrium experiments, as seen in the digital elevation models. During these experiments, the export fractions for both fine and coarse material were relatively low, implying that these grain size classes were preferentially used for the construction of bedforms. On the other hand, in the other fed experiments the export fractions for fine sediment were very high, such that more fine sediment was exported from the channel than imported. This result suggests that fine material is not used for bedform construction once they have matured. Therefore, it can be posited that a coarse mixture of sediment could help enlarge and strengthen bedforms such as pools and riffles. Riffles in particular form at the cross-over points between bars, so the coarse material would likely deposit along the toe of the bars and at the riffles. Particularly valuable for sites like Wilket Creek, where riffles are sometimes removed as a result of floods.

The hypsometric relationships provide insight to erosion and deposition in the vertical direction. During the third and fourth equilibrium experiments, the higher elevation areas reached their final thicknesses after the third experiment, while the lower elevation areas continued to grow throughout the fourth. The possible explanation for this phenomenon may involve an active elevation of deposition which reaches a point where sediment that is deposited is no longer structurally stable, and slides down the slope of the bar, infilling lower elevation areas. This process would also explain the pattern in erosion during the degradation experiments, where higher elevation areas degraded slower than medium and lower elevation areas. If this mechanism exists, it would be possible to deposit sediment in higher regions with expectations that this sediment will be used for construction at all elevations.

The concept that there are limited active sediment transport zones across the width of a channel is incredibly useful for selecting in-river bedform restoration locations. When restoring fish habitat, for example, placing spawning gravel deposits in locations that lie outside of the active transport zone

will result in their eventual degradation, as there is no upstream supply. Estimating the path that sediment will take as it travels downstream will allow for strategic placing of deposits, given that the upstream sediment supply contains the grain size classes of interest. If this is the case, the placed deposits have a chance of replenishment, potentially increasing the lifespan of restoration. Sediment augmentation as a replacement for bedform reconstruction is more efficient because it employs a nature-based solution, working together with the natural environment to improve the structural integrity of channels. A significant drawback of nature-based solutions is the time it takes for them to become established in the area of interest. Geological processes, such as pool-riffle development, occur over extremely long periods of time, so it is not guaranteed that a given restoration design will act as quickly as instream bedform reconstruction. However, with the latter method, long term success is not guaranteed, and the river may revert back to its original state.

Chapter 6 Conclusion

This study used a physical, 1:40 scale model of a creek in Toronto to investigate how sediment is routed through bends and pool-riffle systems. Various experiments were performed in the analysis, beginning with fed, steadily flowing experiments, unfed triangular hydrographs (storms), fed, and steadily flowing experiments between storms that effectively reset the bed (resets). Several methods of observation were utilized, including topographic analysis, storage monitoring, sediment export analysis, hypsometric analysis, and particle tracking under UV-light. Existing theories regarding mechanisms behind pool-riffle maintenance were introduced, including the velocity reversal theory, the sediment routing theory, flow convergence theories, and a particle deflection theory.

Results from this study were mostly consistent with those from Peirce et al. (2021). Discrepancies between results may be due to difference sampling frequencies. The results produced by analysing the active zones of sediment transport suggested that sediment is not routed through pools and towards the outside bank of bends during storm events, as posited by Keller and Turowski, and instead follow the valley trend as they ascended the inner bank's point bar, as depicted by Milan's theory of sediment routing and MacWilliams' theory of flow convergence. Active sediment transport zones were determined to be limited to areas covered with alluvium. The widths of active transport zones increased laterally over connective riffle patches as discharge increased. Export fractions combined with hypsometry curves indicate that, in a state of net sediment loss, an erosive front travels downstream over the span of hours, causing aggradation to occur in front of the sediment pulse. Upstream of the initial front, the rearranged bed is stripped of fines. This phenomenon was observed in the lower regions of bars.

Suggestions for restorative practices were provided based off the study's analyses. Steady degradation of the bed due to a decrease in sediment supply may result in a more turbid river, as armour layers are stripped away to reveal fines. Additionally, adding fines to a river will likely not result in bedform development. Therefore, the type of material used in artificial deposits or other augmentation strategies should be coarse in relation to the grain size distribution in the channel, and deposits should be placed in active sediment transport zones. Considering the relative location of paths within the river bend, it is theorized that deposits placed within these zones will have a longer lifespan, as they will be replenished from upstream material. Based off of results from this thesis, utilizing sediment augmentation as a replacement for bedform reconstruction may improve the lifetime and efficacy of restoration projects. Instead of constructing in rivers, providing rivers with the materials necessary for a robust and functional bed morphology is the only way to ensure that restorative efforts are effective. These types of designs illustrate the effectiveness of nature-based solutions and lessen adverse anthropogenic impacts.

References

AECOM. (2011). *Wilket Creek Geomorphic Systems Master Plan - Appendix B: Hydraulic Study*.

Agisoft. (2023). *Agisoft photo solutions*. Retrieved from https://www.agisoft.com/downloads/installer/

Bankert, A. R., & Nelson, P. A. (2018). Alternate bar dynamics in response to increases and decreases of sediment supply. *Sedimentology*, *65*(3), 702–720. https://doi.org/10.1111/sed.12399

Bayat, E., Rodríguez, J. F., Saco, P. M., de Almeida, G. A. M., Vahidi, E., & García, M. H. (2017). A tale of two riffles: Using multidimensional, multifractional, time-varying sediment transport to assess self-maintenance in pool-riffle sequences. *Water Resources Research*, *53*(3), 2095–2113. https://doi.org/10.1002/2016WR019464

Bevan, V., MacVicar, B., Chapuis, M., Ghunowa, K., Papangelakis, E., Parish, J., & Snodgrass, W. (2018). Enlargement and evolution of a semi-alluvial creek in response to urbanization. *Earth Surface Processes and Landforms*, *43*(11), 2295–2312. https://doi.org/10.1002/esp.4391

Blanckaert, K. (2011). Hydrodynamic processes in sharp meander bends and their morphological implications. *Journal of Geophysical Research: Earth Surface*, *116*(1). https://doi.org/10.1029/2010JF001806

Booker, D. J., Sear, D. A., & Payne, A. J. (2001). Modelling three-dimensional flow structures and patterns of boundary shear stress in a natural pool–riffle sequence. *Earth Surface Processes and Landforms*, *26*, 553–576. https://doi.org/10.1002/esp.210

Byrne, C. F., Pasternack, G. B., Guillon, H., Lane, B. A., & Sandoval-Solis, S. (2021). Channel constriction predicts pool-riffle velocity reversals across landscapes. Geophysical Research Letters, 48, e2021GL094378. https://doi. org/10.1029/2021GL094378

Caamaño, D., Goodwin, P., Buffington, J. M., Liou, J. C. P., & Daley-Laursen, S. (2009). Unifying criterion for the velocity reversal hypothesis in gravel-bed rivers. *Journal of Hydraulic Engineering*, *135*(1), 66–70. https://doi.org/10.1061/(ASCE)0733-9429(2009)135:1(66)

Chartrand, S. M., Jellinek, A. M., Hassan, M. A., & Ferrer-Boix, C. (2018). Morphodynamics of a Width-Variable Gravel Bed Stream: New Insights on Pool-Riffle Formation From Physical Experiments. *Journal of Geophysical Research: Earth Surface*, *123*(11), 2735–2766. https://doi.org/10.1029/2017JF004533

Church, M., & Hassan, M. A. (2002). Mobility of bed material in Harris Creek. Water Resources Research, 38(11), 1237.

Clayton, J. A., and J. Pitlick (2007), Spatial and temporal variations in bed load transport intensity in a gravel bed river bend, Water Resour. Res., 43, W02426, doi:10.1029/2006WR005253.

Czapiga, M. J., Smith, V. B., Nittrouer, J. A., Mohrig, D., & Parker, G. (2015). Internal connectivity of meandering rivers: Statistical generalization of channel hydraulic geometry. *Water Resources Research*, *51*(9), 7485–7500. https://doi.org/10.1002/2014WR016133

Dashtpeyma, H., & MacVicar, B. J. (2023). Plunging Flow and Coherent Turbulent Structures in a Straight Pool-Riffle. *Journal of Geophysical Research: Earth Surface*, *128*(6), e2022JF007034. https://doi.org/https://doi.org/10.1029/2022JF007034

de Almeida, G. A. M., & Rodríguez, J. F. (2011). Understanding pool-riffle dynamics through continuous morphological simulations. *Water Resources Research*, *47*(1). https://doi.org/10.1029/2010WR009170

Einstein, H. A., & Harder, J. A. (1954). Velocity distribution and the boundary layer at channel bends. *Eos, Transactions American Geophysical Union*, *35*(1), 114–120. https://doi.org/10.1029/TR035i001p00114

Frostick, L. E., McLelland, S. J., & Mercer, T. G. (Eds.). (2011). *Users guide to physical modelling and experimentation: Experience of the HYDRALAB network*. CRC Press.

Gardner, T., Ashmore, P., & Leduc, P. (2018). Morpho-sedimentary characteristics of proximal gravel braided river deposits in a Froude-scaled physical model. *Sedimentology*, *65*(3), 877–896. https://doi.org/10.1111/sed.12409

Hassan, M. A., & Church, M. (2000). Experiments on surface structure and partial sediment transport on a gravel bed. Water Resources Research, 36(7), 1885-1895.

Hassan, M. A., Radić, V., Buckrell, E., Chartrand, S. M., & McDowell, C. (2021). Pool-Riffle Adjustment Due to Changes in Flow and Sediment Supply. *Water Resources Research*, *57*(2). https://doi.org/10.1029/2020WR028048

Helm, C., Hassan, M. A., & Reid, D. (2020). Characterization of morphological units in a small, forested stream using close-range remotely piloted aircraft imagery. *Earth Surface Dynamics*, *8*(4), 913–929. https://doi.org/10.5194/esurf-8-913-2020

Heyman, J. (2019). TracTrac: A fast multi-object tracking algorithm for motion estimation. *Computers and Geosciences*, *128*, 11–18. https://doi.org/10.1016/j.cageo.2019.03.007

Julien, P. Y. (2002). River mechanics. Cambridge: Cambridge University Press

Kashyap, S., Constantinescu, G., Rennie, C. D., Post, G., Townsend, R. (2012). Influence of Channel Aspect Ratio and Curvature on Flow, Secondary Circulation, and Bed Shear Stress in a Rectangular Channel Bend. *Journal of Hydraulic Engineering*, *138*(12), 1045–1059. https://doi.org/10.1061/(ASCE)HY.1943-7900.0000643

Keller, E. A. (1971). Areal sorting of bed-load material: The hypothesis of velocity reversal. *Bulletin of the Geological Society of America*, *82*(3), 753–756. https://doi.org/10.1130/0016-7606(1971)82[753:ASOBMT]2.0.CO;2

Leduc, P., Peirce, S., & Ashmore, P. (2019). Short communication: Challenges and applications of structure-from-motion photogrammetry in a physical model of a braided river. *Earth Surface Dynamics*, *7*(1), 97–106. https://doi.org/10.5194/esurf-7-97-2019

Leopold, L. B., & Wolman, M. G. (1960). River meanders. *Bulletin of the Geological Society of America*, *71*(6), 769–793. https://doi.org/10.1130/0016-7606(1960)71[769:RM]2.0.CO;2

Lisle, T. (1979). A sorting mechanism for a riffle-pool sequence. *Bulletin of the Geological Society of America*, *90*(7 PART II), 1142–1157. https://doi.org/10.1130/GSAB-P2-90-1142

Lisle, T. E. (1982). Effects of aggradation and degradation on riffle-pool morphology in natural gravel channels, northwestern California. *Water Resources Research*, *18*(6), 1643–1651. https://doi.org/10.1029/WR018i006p01643

MacVicar, B. J., & Rennie, C. D. (2012). Flow and turbulence redistribution in a straight artificial pool. *Water Resources Research*, *48*(2). https://doi.org/10.1029/2010WR009374

MacVicar, B. J., Rennie, C. D., & Roy, A. G. (2010). Discussion of "Unifying criterion for the velocity reversal hypothesis in gravel-bed rivers" by D. Caamaño, P. Goodwin, J. M. Buffington, J. C. P. Liou, and S. Daley-Laursen. *Journal of Hydraulic Engineering*, *136*(8), 550–552. https://doi.org/10.1061/(ASCE)HY.1943-7900.0000120

MacVicar, B. J., & Roy, A. G. (2007). Hydrodynamics of a forced riffle pool in a gravel bed river: 1. Mean velocity and turbulence intensity. *Water Resources Research*, *43*(12). https://doi.org/10.1029/2006WR005272

MacVicar, B., & Thompson, D. (2023). The diversity of pool-riffle morphologies. *Geomorphology*, *440*, 108868. https://doi.org/https://doi.org/10.1016/j.geomorph.2023.108868

MacWilliams Jr., M. L., Wheaton, J. M., Pasternack, G. B., Street, R. L., & Kitanidis, P. K. (2006). Flow convergence routing hypothesis for pool-riffle maintenance in alluvial rivers. *Water Resources Research*, *42*(10). https://doi.org/10.1029/2005WR004391

Milan, D. J. (2013). Sediment routing hypothesis for pool-riffle maintenance. *Earth Surface Processes and Landforms*, *38*(14), 1623–1641. https://doi.org/10.1002/esp.3395

Morgan, J. A., Brogan, D. J., & Nelson, P. A. (2017). Application of Structure-from-Motion photogrammetry in laboratory flumes. *Geomorphology*, *276*, 125–143. https://doi.org/10.1016/j.geomorph.2016.10.021

Morgan, J. A., & Nelson, P. A. (2021). Experimental investigation of the morphodynamic response of riffles and pools to unsteady flow and increased sediment supply. *Earth Surface Processes and Landforms*, *46*(4), 869–886. https://doi.org/10.1002/esp.5072

Montgomery, D. R., & Buffington, J. M. (1997). Channel-reach morphology in mountain drainage basins. *GSA Bulletin*, *109*(5), 596–611. https://doi.org/10.1130/0016-7606(1997)109<0596:CRMIMD>2.3.CO;2

Ottevanger, W., Blanckaert, K., & Uijttewaal, W. S. J. (2012). Processes governing the flow redistribution in sharp river bends. *Geomorphology*, *163–164*, 45–55. https://doi.org/https://doi.org/10.1016/j.geomorph.2011.04.049

Papangelakis, E., & MacVicar, B. (2020). Process-based assessment of success and failure in a constructed riffle-pool river restoration project. *River Research and Applications*, *36*(7), 1222–1241. https://doi.org/https://doi.org/10.1002/rra.3636

Papangelakis, E., Welber, M., Ashmore, P., & MacVicar, B. (2021). Controls of alluvial cover formation, morphology and bedload transport in a sinuous channel with a non-alluvial boundary. *Earth Surface Processes and Landforms*, *46*(2), 399–416. https://doi.org/10.1002/esp.5032

Parker, G., & Toro-Escobar, C. M. (2002). Equal mobility of gravel in streams: The remains of the day. Water Resources Research, 38(11), 1264.

Peirce, S., MacVicar, B. J., Papangelakis, E., Vervynck, L., & Ashmore, P. (2021). Experiments on restoring alluvial cover using gravel augmentation in a variable width channel with irregular meanders. *Geomorphology*, *379*. https://doi.org/10.1016/j.geomorph.2020.107585

Polvi, L. E. (2021). Morphodynamics of Boulder-Bed Semi-Alluvial Streams in Northern Fennoscandia: A Flume Experiment to Determine Sediment Self-Organization. *Water Resources Research*, *57*(3), e2020WR028859. https://doi.org/https://doi.org/10.1029/2020WR028859

Pospíšilík, Š., & Zachoval, Z. (2023). Discharge coefficient, effective head and limit head in the Kindsvater-Shen formula for small discharges measured by thin-plate weirs with a triangular notch. *Journal of Hydrology and Hydromechanics*, *71*(1), 35–48. https://doi.org/10.2478/johh-2022-0040

Redolfi, M., Tubino, M., Bertoldi, W., & Brasington, J. (2016). Analysis of reach-scale elevation distribution in braided rivers: Definition of a new morphologic indicator and estimation of mean quantities. *Water Resources Research*, *52*(8), 5951–5970. https://doi.org/10.1002/2015WR017918

Sawyer, A. M., Pasternack, G. B., Moir, H. J., & Fulton, A. A. (2010). Riffle-pool maintenance and flow convergence routing observed on a large gravel-bed river. *Geomorphology*, *114*(3), 143–160. https://doi.org/10.1016/j.geomorph.2009.06.021

State of Maine Department of Environmental Protection (DEP). (2007). Rapid Geomorphic Assessment Key. Retrieved from: https://dep.wv.gov/WWE/getinvolved/sos/Documents/More/RGA_PictureKey(Maine).pdf

Stone, M., Emelko, M. B., Droppo, I. G., & Silins, U. (2011). Biostabilization and erodibility of cohesive sediment deposits in wildfire-affected streams. *Water Research*, *45*(2), 521–534. https://doi.org/https://doi.org/10.1016/j.watres.2010.09.016

Tal, M., & Paola, C. (2010). Effects of vegetation on channel morphodynamics: results and insights from laboratory experiments. *Earth Surface Processes and Landforms*, *35*(9), 1014–1028. https://doi.org/https://doi.org/10.1002/esp.1908

Thompson, D.M., 2018. Pool–Riffle Sequences. Reference Module in Earth Systems and Environmental Sciences.

Turowski, J. M. (2018). Alluvial cover controlling the width, slope and sinuosity of bedrock channels. *Earth Surface Dynamics*, *6*(1), 29–48. https://doi.org/10.5194/esurf-6-29-2018

Vahidi, E., Rodríguez, J. F., Bayne, E., & Saco, P. M. (2020). One flood is not enough: Pool-riffle self-maintenance under time-varying flows and nonequilibrium multifractional sediment transport. Water Resources Research, 56, e2019WR026818. https:// doi.org/10.1029/2019WR026818

White, J. Q., Pasternack, G. B., & Moir, H. J. (2010). Valley width variation influences riffle-pool location and persistence on a rapidly incising gravel-bed river. *Geomorphology*, *121*(3–4), 206–221. https://doi.org/10.1016/j.geomorph.2010.04.012

Wilcock, P. R., & McArdell, B. W. (1993). Surface-based fractional transport rates: Mobilization thresholds and partial transport of a sand-gravel sediment. *Water Resources Research*, *29*(4), 1297–1312. https://doi.org/https://doi.org/10.1029/92WR02748

Wilcock, P. R., Kondolf, G. M., Matthews, W. V. G., & Barta, A. F. (1996). Specification of sediment maintenance flows for a large gravel-bed river. *Water Resources Research*, *32*(9), 2911–2921. https://doi.org/10.1029/96WR01627